Satellite-based modelling of vegetation productivity in the Netherlands.

Net Primary Productivity downscaling MODIS algorithm.

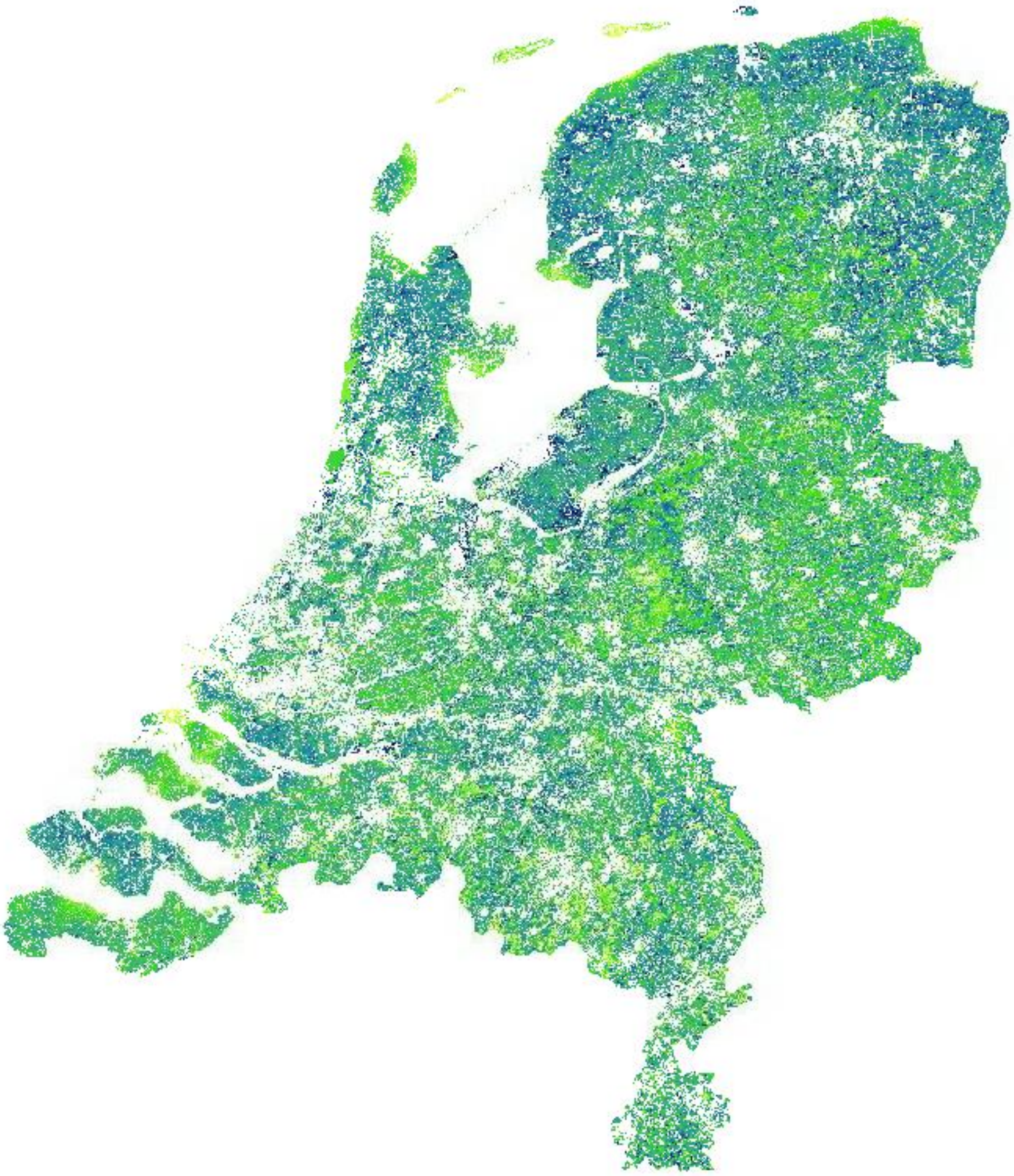

Author:

Pedro Lorenzo Cruz

Master Student

Dept. of Environmental Sciences, Radboud University, Nijmegen

Abstract

Carbon accounting has gained importance during the last years due to the current transition to a circular economy. These accounts can be expressed as supply of several ecosystem services such as biomass production, biomass for energy or climate regulation. As ecosystem services has been established as a key tool in management and governance, precise information of carbon fluxes is needed to support the valuation of ecosystem services leading sustainable policies.

With the aim of producing sound information for several ecosystem services, this study focus on the process that triggers these service, which is the vegetation carbon uptake and storage of carbon. Many different approaches have reported Gross Primary Productivity and Net Primary Productivity quantifying the amount of dry carbon fixed by vegetation. Sparse measurements provide insufficient data to be relevant for policy, and most of the existing models produce coarse information both in the temporal and spatial scales.

This study has built a satellite-based model to provide monthly Net Primary Productivity data at 10m resolution for the Netherlands. The model is conceptually based in MODIS algorithms, whose products offer good productivity estimates with a resolution 500m. Our model includes higher resolution inputs to improve consistently other approaches, offering high quality spatial information of 10m. Monthly products allow us to track seasonality revealing climatic effects, management practices or land cover change under all the vegetation types of the Netherlands.

Continuous spatial and temporal data, output resolutions higher than current process-based models, and decreasing uncertain parameters are measures needed for a robust assessment of vegetation productivity involving the entire non-urban surface of the Netherlands.

Declaration

This study is part of a thesis for Master Studies in Biology in Radboud University. The research has been undertaken in the Centre for Sustainability, Environment and Heallth at the Netherlands National Institute for Public Health and the Environment as an internship project during 6 months under the supervision of Dr. R. Remme.

TABLE OF CONTENTS

1 – Introduction

1.1 - Ecosystem services

In the last few decades the concept of ecosystem services (ES) had gained much attention in the scientific community and has been established as a key tool in management and governance (Costanza et al., 1997; De Groot et al., 2002; Millennium Ecosystem Assessment, 2005). One of the most commonly definitions used is the description by the Millennium Ecosystem Assessment (2005), which states that ecosystem services are “the benefits people obtain from ecosystems directly or indirectly”. Examples of these benefits are for instance food, timber, drinking water, climate regulation, or cultural values. (Wallace, 2007).

Quantification of ES requires modelling and monitoring strategies to compute and determine a wide range of ES offered, but also the synergies and trade-offs between them (Burkhard et al., 2013; Braat and de Groot, 2012; Crossman et al., 2013). Considering the social and environmental challenges our planet currently faces, underlining ES contributions to climate change mitigation and societal benefits has high importance. A precise assessment of these two fields is crucial to face one of the mayor socio-economic and environmental drivers of change globally: the rapid land cover change arising from a fast growing population (UNEP, 2000).

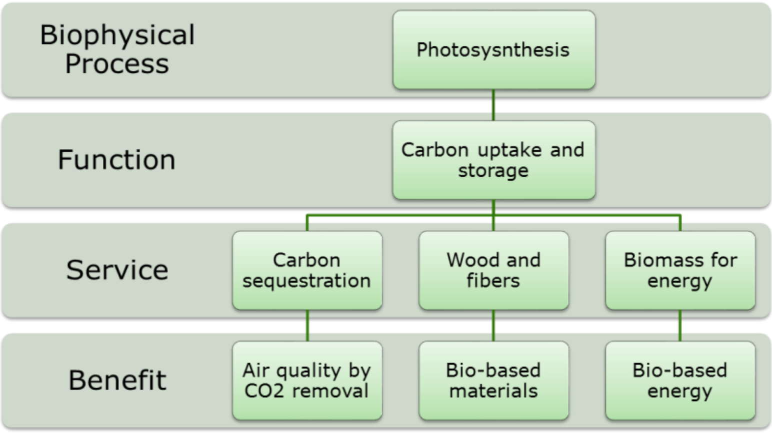

Figure 1: Ecosystem service cascade framework applied for this case study

Land cover changes can affect inundation regime, temperature, humidity, wind, air quality, radiation, and precipitation altering the carbon flows between the vegetation and the atmosphere (Lal, 2008; Costanza et al., 2014). Thus, a logical consequence is that one of the most studied ES globally is carbon sequestration due to its applications dealing with climate change (Crossman et al. 2013). The supply of this service is defined by the capability of the vegetation to capture and store carbon through photosynthesis. Therefore, quantifying photosynthetic activity provide fundamental information of the amounts of carbon captured and released by vegetation to estimate carbon sequestration. Additionally, quantifying carbon flows also leaves the possibility to asses other relevant ES such as wood production, biomass for energy, or crop production (Figure 1). Despite its importance, a framework to account for carbon flows in biomass has not been addressed yet at a national scale using high spatial and temporal resolution. A robust methodology to quantify above- and below-ground carbon uptake and storage accurately in the mid-long term is needed to include carbon related ES into assessment and accounting processes for natural capital, that inform decision making processes and valuation from environmental and efficiency perspectives.

1.2 - Carbon Cycle

One of the main features of the carbon cycle is its importance as Earth's climate regulator, by controlling atmospheric carbon dioxide levels. Carbon dioxide is an important greenhouse gas responsible for global warming and ocean acidification (IPCC, 2014). The release of atmospheric carbon has become a topic of general interest because of the increasing amounts of CO_2 our planet is faced with. The CO_2 concentration in the atmosphere is increasing at a rate of 2 ppm per year, which means a growth of 0.52% annually (Lal, 2008), even though the CO_2 uptake trends from 2000 to present are still under debate (Zhao and Running, 2010; Samanta et al., 2011; Ahlstrom et al., 2012).

The carbon cycle works as a system controlled by different pools of carbon and fluxes transferring carbon between them, as represented in *Figure 2*. The rate at which carbon is absorbed by vegetation through photosynthesis is also known as Gross Primary Productivity (GPP) (Chapin et al., 2006). GPP has a key role in the carbon cycle because it comprises the largest CO2 flux estimated at 120 megatons of carbon per year globally (Beer et al., 2010).

Net Primary Productivity (NPP) is defined as the dry matter production by vegetation. It can be calculated as the difference between GPP and autotrophic respiration or, in other words, the rate at which vegetation captures CO_2 from the atmosphere minus the rate at which it is released by photosynthesis (Melillo et al., 1993; Ito, 2011).

NPP rates over Europe have shown an increase of 4.40% during the last two decades

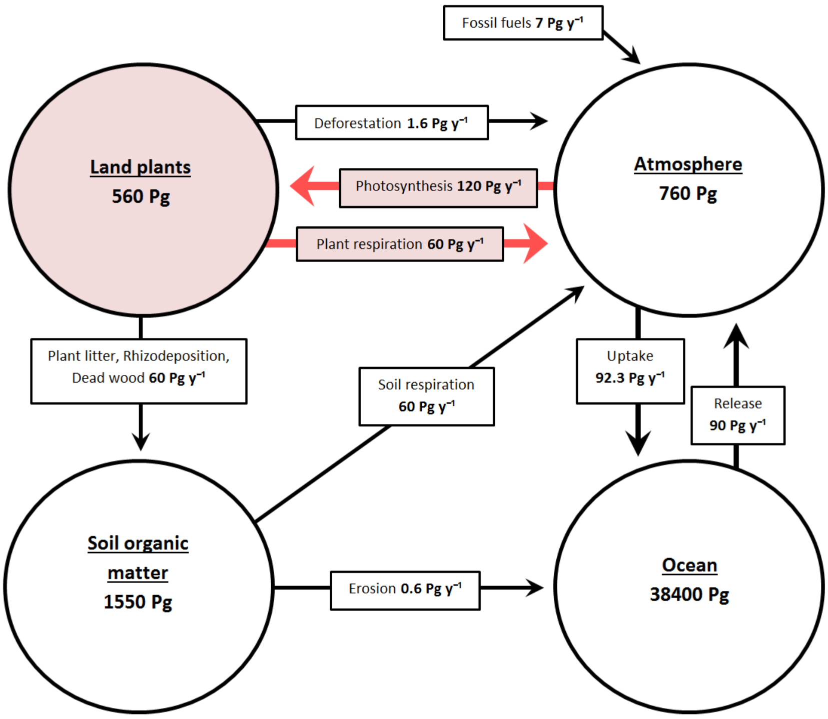

Figure 2: Global carbon pools and their annual fluxes with field of interest in red. Flowchart adapted from Lal (2008) and IPCC (2007).

of 20th century (De Fries et al., 1999), becoming the continent with the highest increase in NPP due to the land use changes but also the reduction of climate constraints increasing temperatures and solar radiation (Nemani et al., 2003). Forest and non-forest conversion to cropland are the most relevant land use changes explaining this trend.

NPP is considered to be a precise indicator for climate change and for ecological and environmental monitoring and a good tool to measure several ES such as biomass production, supply of materials, supply of biomass for energy, carbon sequestration or athmospheric regulation (Matsushita and Tamura, 2002; Gower et al., 1999, Running et al, 2004, Imhoff et al., 2004).

1.3 - Satellite imagery

Broad-scale vegetation analysis through satellite imagery has overcome the empirical approach and the ground process-based model measuring GPP and NPP during the last years. The main reasons are the complexity to measure these variables in-situ from the empirical models, and the lack of spatial coverage from the ground process-based model.

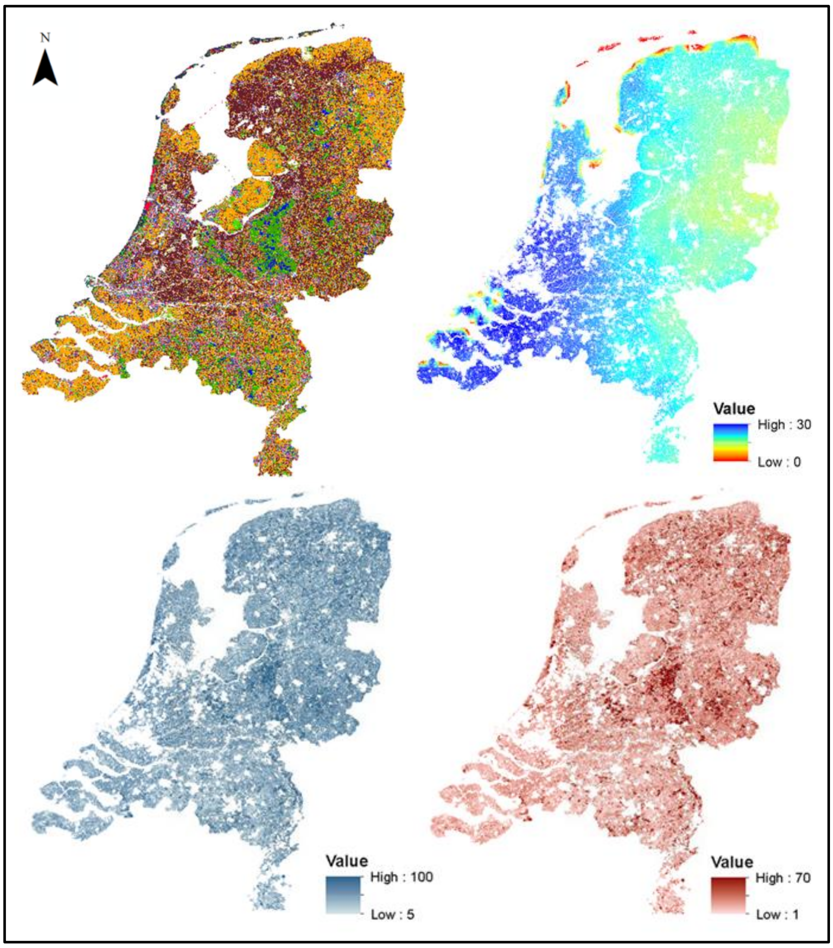

Figure 3: Map of the Netherlands including (1) Land cover EU_NL from CBS, (2) DSSF from MSG, (3) FPAR from MOD15, and (4) LAI from MOD15

One of the most reliable GPP and NPP estimations is offered by MODerate resolution Imaging Spectroradiometer (MODIS) since the year 2000. MODIS products (MOD17) provide continuous global estimates of GPP and NPP spatially and temporally, with a 500m resolution (Running et al 2004, Zhao et al 2010). MODIS combines an ecophysiological modelling approach taking into account satellite reflectance measurements in an 8-day basis from the TERRA and AQUA satellites (Figure 3), daily climate measurements and some fixed parameters from the Biome-Property-Look-Up-Table, which is included in the Appendix 1, and includes values derived from the BIOME-BGC model (Thornton, 2003; Zhao et al., 2005).

Even though NPP estimations commonly include great uncertainty, MOD17 algorithm has shown reliable estimates decreasing consistently uncertainty on the last products, which have also been validated in Europe (Neumann et al., 2015; Moreno et al., 2015). The main source of uncertainty originates from cloud contaminated satellite reflectance products (LAI and FPAR). Currently, cloud masks have been applied and the algorithm also depends on daily meteorological measurements that allow filling the contaminated data gaps (Running et al 2004, Zhao et al 2010).

Nonetheless, MOD17 algorithm provide GPP and NPP products with a resolution of 500m offering good estimates globally but lacking spatial resolution in the regional and local scale. Including higher resolution input datasets would improve consistently the products offering high quality spatial information. The land cover map is the parameter with the highest influence on the algorithm, thus improvements in land cover classifications leave the possibility to downscale substantially the current resolution of 500m from MOD17 products.

1.4 - Aim of the project

A high resolution NPP model has been developed for the Atlas of Natural Capital (ANK) at the Netherlands National Institute for Public Health and the Environment (RIVM) with the goal of contributing to map ES at high both spatial and temporal resolution in the Netherlands. With this purpose, we have built a consistent methodology to quantify the vegetation productivity and carbon uptake in the Netherlands. It focuses on improving the current carbon accounts of the country through GPP and NPP accounts from satellite imagery. Satellite-based data allows quantification of biophysical parameters enhancing both spatial and temporal scales of carbon trends. From the spatial perspective, this model provides outputs of 10m resolution, significantly improving current global and regional approaches. From the temporal perspective, monthly data is obtained reporting seasonal patterns, and addressing anomalies due to intensive management or climatic events. The development of this biophysical-modelling methodology through remote sensing provide novel information that can be used for assessing carbon sequestration and biomass production with different purposes such as agriculture, grasslands for livestock or wood production. This information contributes to the national carbon accounts of the Netherlands and it will help managers and policy makers to secure a sustainable ecosystem management in decision making processes.

At present, models accounting for carbon sequestration in the Netherlands have not linked spatio-temporal variations in carbon accounting, hence the aims of this study are: (1) biophysically quantify GPP and NPP in the Netherlands for the year 2013; (2) analyse spatial variability across the Dutch provinces; (3) report monthly variations in the year 2013; (4) make a descriptive analysis comparing this methodology with others; and (5) provide recommendations for further carbon accounts.

2 – Methods

Vegetation productivity for the Netherlands has been estimated in 10m resolution. The spatial coverage includes most land cover types, except urban areas, paved surfaces and water bodies. The methodology includes the improvement of the MOD17 algorithm through the construction of a model (Appendix 2) which contain reflectance variables from MODIS satellite products such as Leaf Area Index (LAI) and Fraction of Absorbed Photosynthetically Active radiation (FAPAR); constant parameters from Biome-Property-Look-Up-Table (BPLUT); data of Downward Shortwave Surface Flux radiation (DSSF) from METEOSAT Second Generation products and land cover information from the recently developed EU_NL map.

The model can be divided in for sub-models to explain separately the products calculated(Figures 4-8). All the steps and parameters (Appendix 3) are explained in detail below.

2.1 – GPP

The first of four models for accounting vegetation productivity has been built to derive Gross Primary Productivity estimations in the Netherlands (Figure 4). The model relies on the existing relations between the light use efficiency (ε) of the different vegetation types and the absorbed photosynthetically active radiation (APAR), based on the method proposed by Monteith (1972):

$$GPP_m = \varepsilon * APAR_m \qquad (1)$$

Where,

GPP *Monthly Gross Primary Productivity;*

ε *Light Use Efficiency;*

APAR *Monthly Absorbed Photosynthetically Active Radiation. Eq. 2;*

m *Month.*

The first term, ε, is a constant value for each land cover type assigned to the land cover map for the Netherlands (EU_NL). EU_NL has been developed by CBS for the year 2013. It includes 23 different land cover classes under an accurate resolution of 10 meters. This map is the pillar of this model because it will define the size of the output. Thus, each pixel of $10m^2$ is given a different treatment according to all the inputs.

Maximum ε values (ε_{max}) are determined by the Look-Up Table (Sala et al., 2000). The values of ε_{max} are derived from simulations with the BIOME-BGC model (Thornton, 2003), which have adjusted its parameters to biome-specific conditions. They represent the photosynthetic activity under optimal conditions (Garbulsky et al., 2010). These values include 11 different land cover types from which 9 are used in our model, excluding land cover types that do not exist currently in the Netherlands. The land cover conversion from the Look-Up Table to CBS land cover types is defined in Appendix 4.

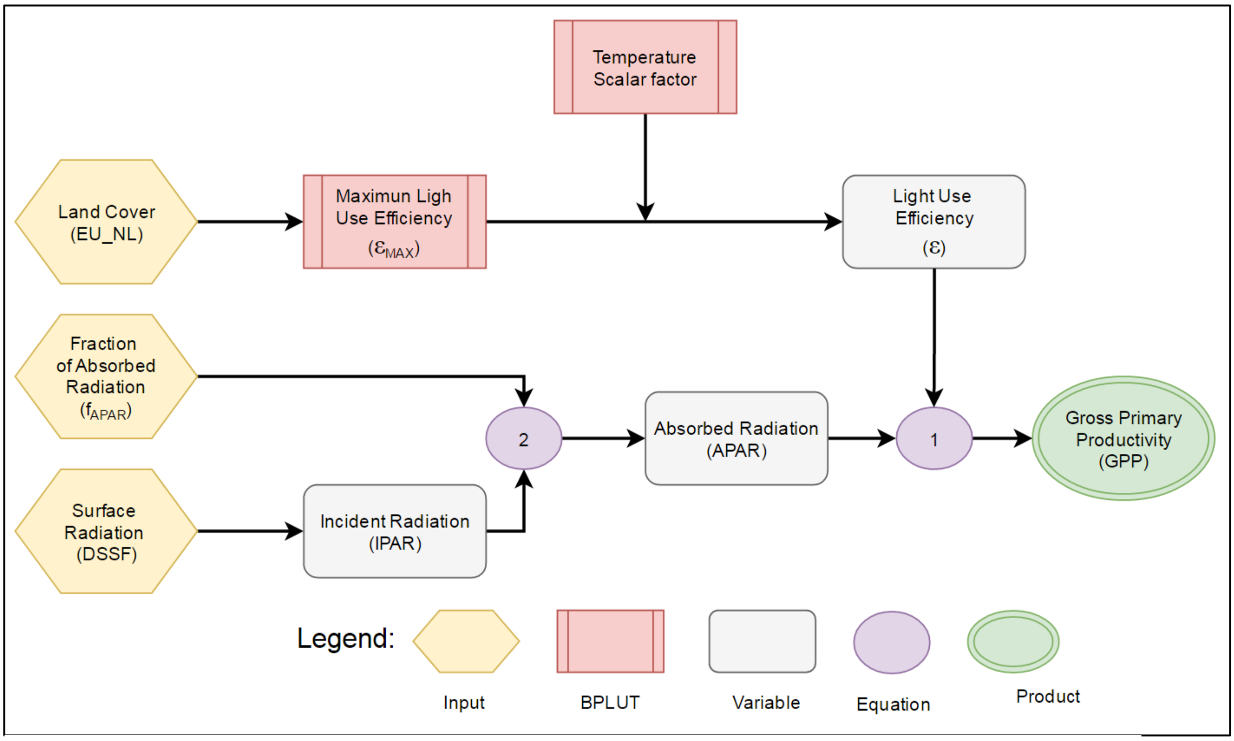

Figure 4: Flowchart for modelling monthly Gross Primary Productivity

The second variable that needs to be calculated is the APAR. Direct satellite measurements of this variable do not exits, then it is calculated as the product between the incident photosynthetically active radiation (IPAR) and the fraction of absorbed photosynthetically active radiation (f_{APAR}), which derived from MODIS reflectance data (Yang et al., 2006) as described:

$$APAR_m = IPAR_m * f_{APAR\,m} \tag{2}$$

Where,

$APAR_m$ *Monthly* Absorbed Photosynthetically Active Radiation;

$IPAR_m$ *Monthly* Incident Photosynthetically Active Radiation;

$f_{APAR\,m}$ *Monthly Fraction of Absorbed Photosynthetically Active Radiation;*

m *Month.*

IPAR measurements are defined as the 45% of the Downward Surface Shortwave Flux radiation (DSSF). DSSF is one of the inputs of this model and refers to the radiative energy in the wavelength interval 0.3 – 4 µm that reach the Earth's surface given in satellite measurements expressed in Joules per square meter per day. This data is recorded by Meteosat Second Generation satellite every 30 minutes according to the solar zenith angle, the cloud cover and the surface albedo (LSA SAF, 2011a). The datasets have been extracted from the data pool of Meteosat platform, which release products in a 3 km resolution at nadir, and 12 spectral channels (Schmetz et al., 2002). Several algorithms are used to account for meteorological circumstances, providing a cloud mask to avoid disturbances in the outputs (LSA SAF, 2011b). These outputs have been composited in monthly intervals.

f_{APAR} is the proportion (dimensionless) of available radiation in the photosynthetically active wavelengths that the canopy absorbs. These datasets are obtained from MODIS satellite in an 8-day interval with a resolution of 500 meter pixel size. It has been widely validated using also cloud masks to avoid data errors (Yan et al., 2016)). These datasets are composited, resampled and stored in monthly basis.

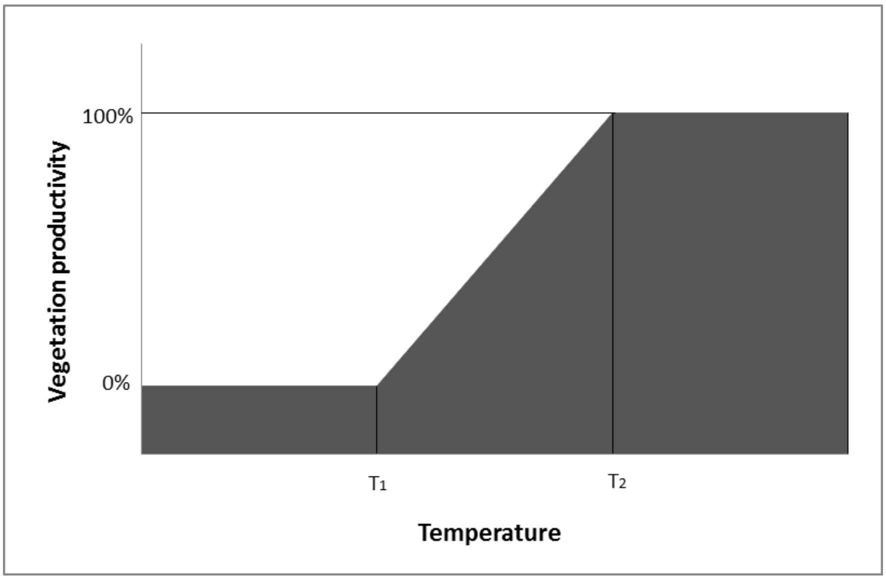

Figure 5: Scalar linear ramp to reduce vegetation productivity with low temperatures

The temperature is also taken into account to attenuate light use efficiency. Using biome-specific values from the BPLUT, we can determine the minimum temperature at which each vegetation type start decreasing its productivity (T2), but also the temperature boundary where vegetation is not productive any more (T1). With this purpose, we have applied a linear scalar factor to reduce final productivity due to temperature stress (Figure 5). The surface temperature data has a strong impact on the model and it was obtained from MODIS data pool (Neumann 2015, Running and Zhao, 2015). Temperature datasets were also validated with a 1 km resolution on a daily basis (Wan et al, 2004). We have built monthly composites to derive the average temperatures for each month of 2013 to account for the loss of productivity for each particular vegetation type due to temperature stress.

Finally, the output from these calculations is the monthly GPP with a resolution of 10 meters. GPP monthly information is given in tons per hectare per year, in a 0.01 scale.

2.2 – Leaves: Mass and Respiration

With the aim of accounting for the carbon released during plant respiration, we firstly built a model to measure the respiration of leaves, and consequently the amount of leaves per pixel (Figure 6). The leaf mass ($Leaf_{MASS}$) can be calculated through the Leaf Area Index (LAI) and the Specific Leaf Area (SLA) as shown:

$$Leaf_{MASS\,m} = LAI_m / SLA_m \qquad (3)$$

Where,

$Leaf_{MASS}$ Mass of leaves;

LAI Leaf Area Index;

SLA Specific Leaf Area;

m Month.

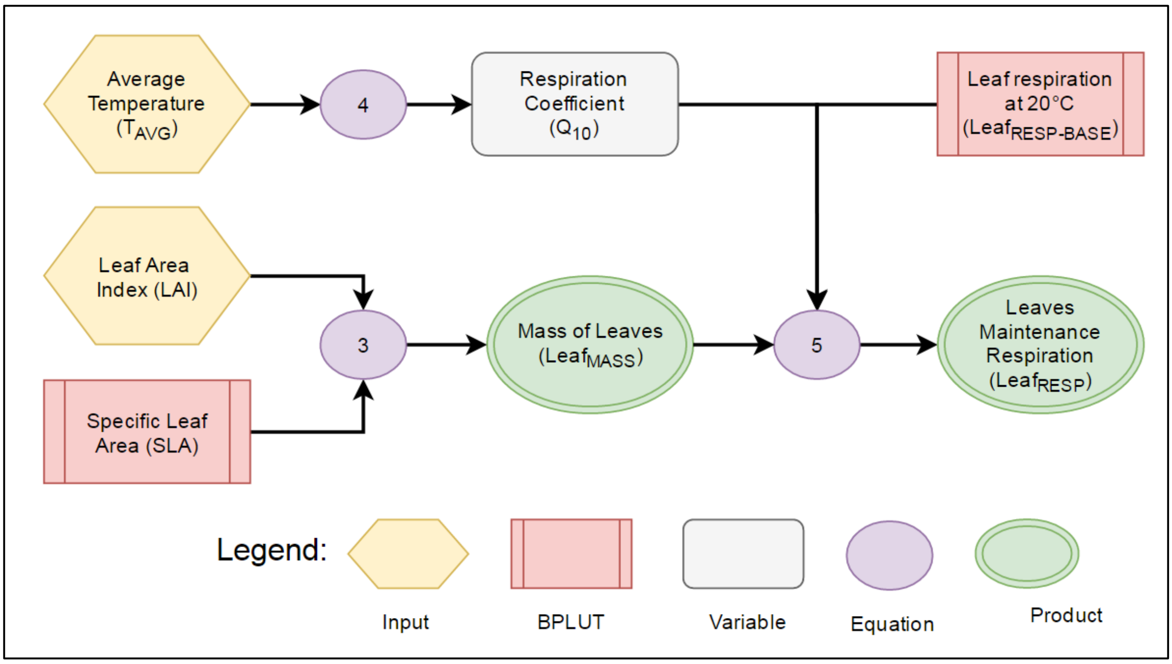

Figure 6: Flowchart for estimating the biomass in leaves and their monthly maintenance respiration

The Leaf Area Index (dimensionless) is the ratio of leaves in vegetation in a given area in the land surface. LAI has been compiled from MODIS reflectance data (Yang et al. 2006), which produces this information with a resolution of 500 meters in 8 day intervals, along with f_{APAR}, and also validated. These datasets are composited into monthly maps of LAI, then resampled and rescaled to our framework units.

The parameter SLA represents the projected leaf area per unit mass of leaf carbon, which is directly involved in the leave's carbon balance. The values of SLA for each vegetation type are subtracted from the BPLUT and its units are square meters per kilogram of carbon.

Once the total amount of leaves in each pixel is estimated in monthly basis, the quantification of carbon released by leave's respiration becomes possible ($Leaf_{RESP}$). The base maintenance respiration of leaves at 20°C ($Leaf_{RESP-BASE}$)can be found in the BPLUT for each land cover type in Kilograms of carbon released per kilograms of carbon content in the leaves per day. To account accurately for maintenance respiration, we also have accounted for the Q_{10} temperature coefficient (Tjoelker et al., 2001). The Q_{10} is commonly used to describe physiological responses to temperature and in this case, it will adjust the results of leave respiration as a function of average monthly temperatures. The value of Q_{10} is described as:

$$Q_{10\,m} = 3.22 - 0.046 * T_{AVG\,m} \tag{4}$$

Where,

Q_{10} *Coefficient for temperature respiration;*

T_{AVG} *Monthly Average Temperature;*

m *Month.*

Then, the maintenance respiration is calculated with this equation:

$$Leaf_{RESP\,m} = Leaf_{MASS\,m} * Leaf_{RESP\text{-}BASE} * Q_{10}\,[(T_{AVG\,m} - 20.0) / 10.0] \quad (5)$$

Where,

$Leaf_{RESP}$ *Amount of carbon resealed by maintenance respiration in leaves;*

$Leaf_{MASS}$ *Mass of leaves;*

$Leaf_{RESP\text{-}BASE}$ *Maintenance respiration of leaves at 20°C;*

Q_{10} *Coefficient for temperature respiration;*

T_{AVG} *Monthly average surface temperature;*

m *Month.*

2.3 – Fine roots and Living wood: Mass and Respiration

To quantify accurately the total amount of carbon released from biomass through respiration we must also consider the respiration of fine roots and woody tissues (Figure 7). First, we determined the mass of fine roots ($Root_{MASS}$) from the ratio of fine roots to the leaf mass ($Root\text{-}Leaf_{RATIO}$) provided in the BPLUT. with the equation:

$$Root_{MASS\,m} = Leaf_{MASS\,m} * Root\text{-}Leaf_{RATIO} \quad (6)$$

Where,

$Root_{MASS}$ *Monthly mass of roots;*

$Leaf_{MASS}$ *Monthly mass of leaves;*

$Root\text{-}Leaf_{RATIO}$ *Ratio from mass of roots and the mass and leaves;*

m *Month.*

Afterwards, we also determined the existing mass of living wood ($Wood_{MASS}$) following the same method, deriving the values from the mass ratio between wood and leaves ($Wood\text{-}Leaf_{RATIO}$) according to the BPLUT. But in this case, wood mass is derived from the maximum leaf mass per pixel during the year ($Leaf_{MASS\text{-}MAX}$). This is meant to consider wood also non-perennial vegetation and assuming constant wood values during the year according to the equation:

$$Wood_{MASS\,m} = Leaf_{MASS\text{-}MAX} * Wood\text{-}Leaf_{RATIO} \quad (7)$$

Where,

$Wood_{MASS}$ *Monthly mass of wood;*

$Leaf_{MASS-MAX}$	*Maximum annual mass of leaves;*
$Wood\text{-}Leaf_{RATIO}$	*Ratio from mass of roots and the mass and leaves;*
m	*Month.*

These results allow to quantify the total existing biomass monthly, and from them we derived the maintenance respiration rates of fine roots ($Root_{RESP}$) and living wood ($Wood_{RESP}$) in the following equations. The BPLUT includes both maintenance respiration terms at 20°C ($Root_{RESP\text{-}BASE}$, $Wood_{RESP\text{-}BASE}$) as well and the Q_{10} parameter, which is assumed to have a constant value of 2 for respiration of wood and roots.

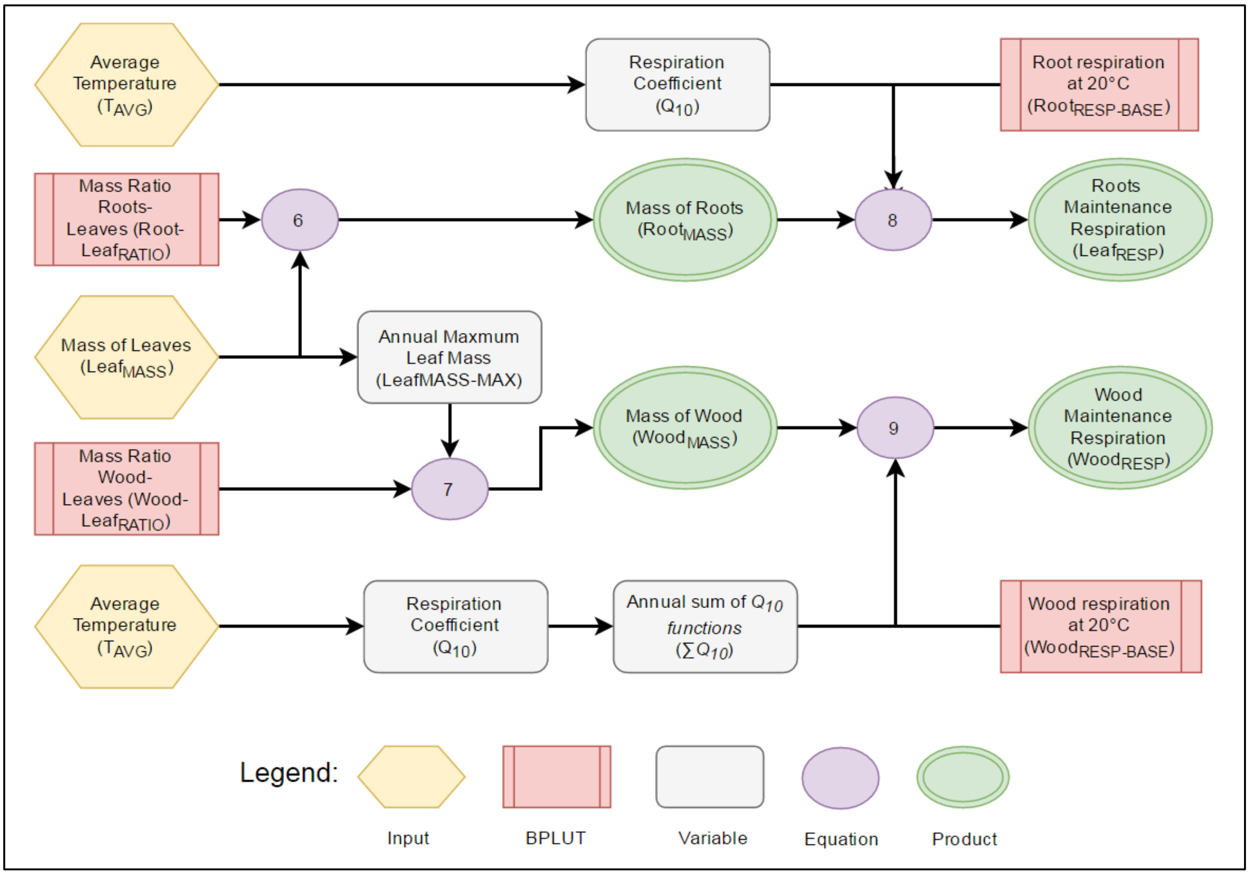

Figure 7: Flowchart for estimating the biomass in fine roots and living wood, and their monthly maintenance respiration

In the case of living wood, the Q_{10} term is considered as the sum of the monthly Q_{10} functions during the year. The equations bellow describe the calculation for root and living wood respiration respectively:

$$Root_{RESP\,m} = Root_{MASS\,m} * Root_{RESP\text{-}BASE} * Q_{10}\,[(T_{AVG\,m} - 20.0) / 10.0] \qquad (8)$$

$$Wood_{RESP\,m} = Wood_{MASS\,m} * Wood_{RESP\text{-}BASE} * \sum Q_{10}\,[(T_{AVG\,m} - 20.0) / 10.0] \qquad (9)$$

Where;

$Root_{RESP}$	*Monthly amount of carbon resealed by maintenance respiration in roots;*
$Root_{MASS}$	*Monthly mass of roots;*
$Root_{RESP\text{-}BASE}$	*Maintenance respiration of roots at 20°C;*

Q_{10} *Coefficient for temperature respiration;*

T_{AVG} *Monthly average surface temperature;*

$Wood_{RESP}$ *Monthly amount of carbon resealed by maintenance respiration in wood;*

$Wood_{MASS}$ *Monthly mass of wood;*

$Wood_{RESP\text{-}BASE}$ *Maintenance respiration of wood at 20°C;*

m *Month.*

2.4 – Net Primary Productivity

Consequently, the total biomass respiration ($Resp_{TOTAL}$) is quantified as the sum from the carbon released by leaves, roots and wood:

$$Resp_{TOTAL\ m} = Leaf_{RESP\ m} + Root_{RESP\ m} + Wood_{RESP\ m} \quad (10)$$

Where,

$Resp_{TOTAL}$ *Monthly amount of carbon resealed by maintenance respiration;*

$Leaf_{RESP}$ *Monthly amount of carbon resealed by maintenance respiration in leaves;*

$Root_{RESP}$ *Monthly amount of carbon resealed by maintenance respiration in roots;*

$Wood_{RESP}$ *Monthly amount of carbon resealed by maintenance respiration in wood;*

m *Month.*

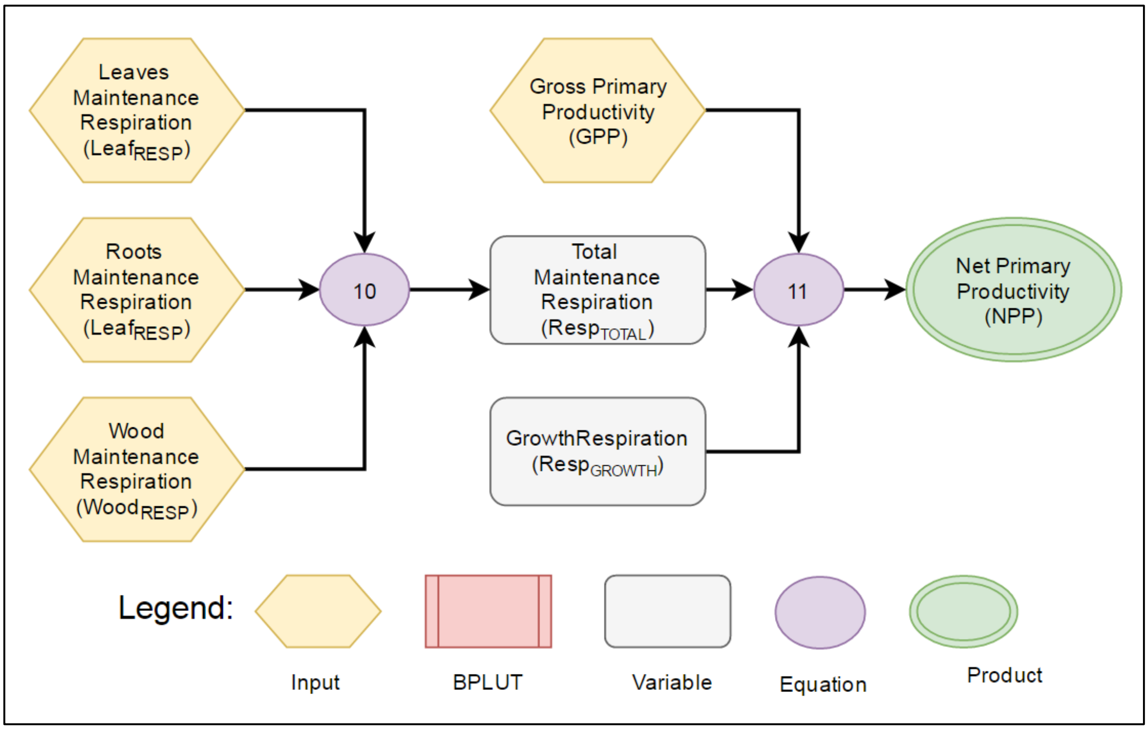

Figure 8: Flowchart for modelling Net Primary Productivity

The Net Primary Productivity is calculated removing the maintenance respiration values, which have been already calculated, and the growth respiration, which have been empirically measured as 25% of the NPP (Ryan 1991, Cannell et al. 2000), from the Gross Primary Productivity (Figure 8). We can derive NPP values according to the equation:

$NPP_m = GPP_m - \mathrm{Resp}_{\mathrm{TOTAL\ m}} - \mathrm{Resp}_{\mathrm{GROWTH\ m}} = GPP_m - \mathrm{Resp}_{\mathrm{TOTAL\ m}} - 0.25NPP_m =>$

$NPP_m = 0.8 * (GPP_m \text{-} \mathrm{Resp}_{\mathrm{TOTAL\ m}})$
(11)

Where,

NPP *Monthly Net Primary Productivity*

GPP *Monthly Gross Primary Productivity*

$Resp_{TOTAL}$ *Monthly amount of carbon resealed by maintenance respiration;*

$Resp_{GROWTH}$ *Monthly amount of carbon resealed by growth respiration;*

m *Month*

2.5 – Validation

Finally, a statistical analysis was performed. Mean, Standard Deviation, Range, Maximum and Minimum, Sum, Majority and Minority, and Median from NPP were calculated for each land cover type at municipality, province and national scales. The analysis includes monthly variations and computes the total carbon stock and the rate of change across the year 2013. This methodology allowed not only a novel satellite quantitative estimation of carbon uptake rates and carbon stocks from vegetation in the Netherlands but also their spatiotemporal development.

The final annual composites were also compared with the MODIS (MOD17A3H) data for 2013, which offer NPP rates at 500m resolution. This comparison was based on average NPP rates distributed according to each land cover class from the CBS classification, allowing to compare MODIS algorithm results with our downscaled products based on the information from a joint model by the Flemish Institute for Technological Research (VITO) and RIVM, and the carbon account of Statistics Netherlands (CBS).

3 – Results

The Netherlands comprise a land surface of 3351 km^2 and this study has analyzed 72.5% (2429 km^2) of its territory, which includes all vegetation types. This surface is responsible of the removal and storage of 976 Mton C from the atmosphere in 2013. During this year, the average Net Primary Productivity of the Netherlands was 3.26 ± 0.64 ton C ha^{-1} y^{-1} (Figure 8). The highest rates were found in Deciduous Forest during the month of July (10.47 ± 2.01 ton C ha^{-1} y^{-1}), while the lowest were recorded in January being approximately 0 for all land cover types. Land cover and seasonality are the main indicators for the variability of vegetation productivity as shown in Appendix 5.

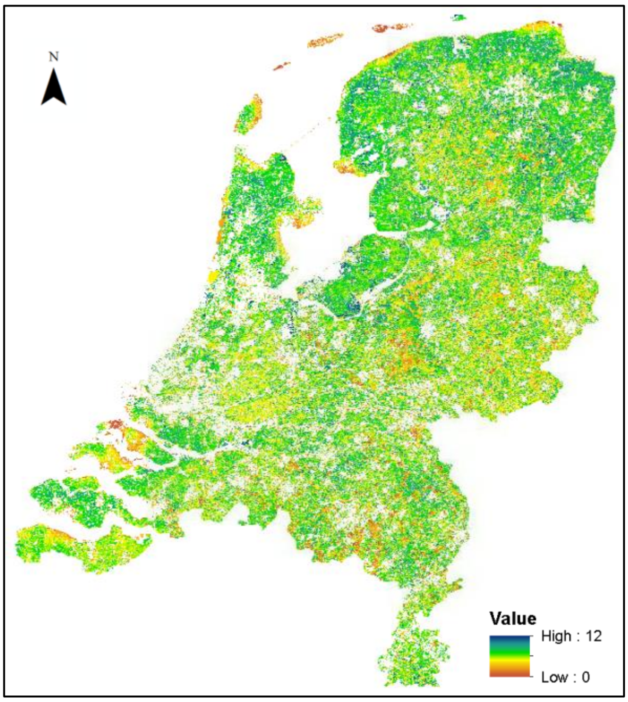

Figure 8: Annual vegetation productivity (ton C m^{-2} y^{-1}) during the year 2013.

3.1 – Land Cover

The monthly Net Primary Productivity rates resulting from the model were analyzed according to the land cover types from the EU_NL map, which are collected in the Appendix 4. The land cover types considered as forested areas (Figure 9) obtained the highest variability in their annual NPP rates for 2013. Between January to March the NPP slightly grew from 0 to 1 ton C ha^{-1} y^{-1}. Forests experienced a sudden increase of their productivity from March to April increasing from 500 to 800% their monthly NPP

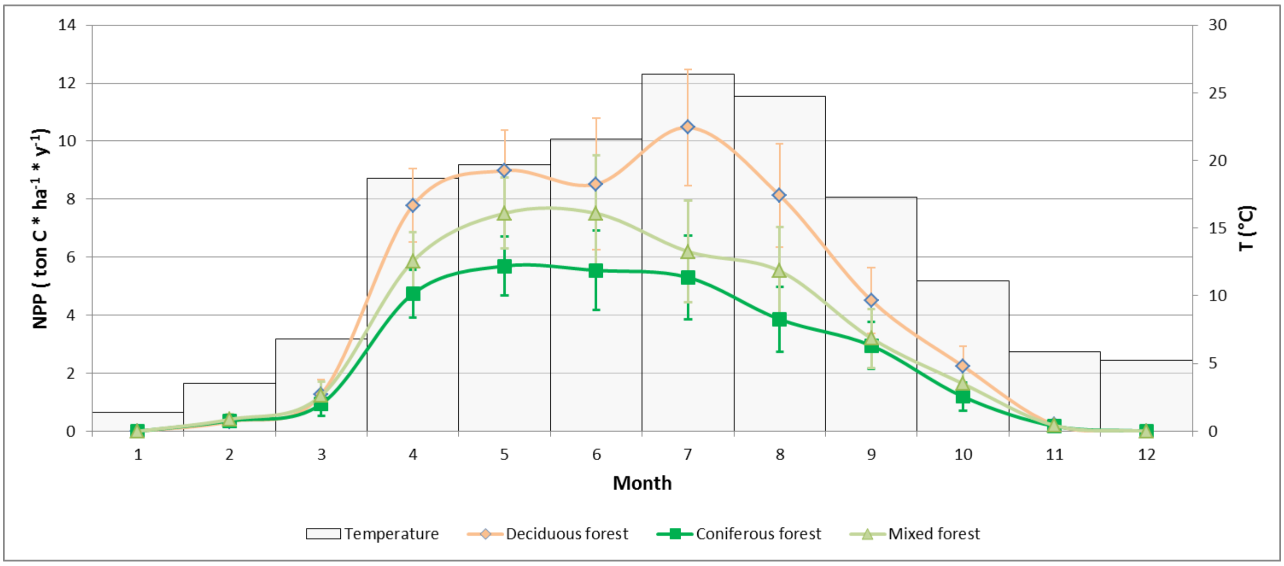

Figure 9: Monthly Net Primary Productivity rates and Temperatures for forest land cover types in the Netherlands during the year 2013.

rates and matching with the highest increase in temperatures. From April to June NPP gained stability followed by increasing NPP rates in July on deciduous forests to 10.47 ± 2.01 ton C ha^{-1} y^{-1} and decreasing in mixed forest to 6.11 ± 1.20 ton C ha^{-1} y^{-1}, corresponding with the maximum yearly temperatures. Afterwards forest productivity declined constantly from July until December. Deciduous forest were the forest class that produced more biomass per area across the year (4.37 ton C ha^{-1} y^{-1}) reaching its upper value in July, while NPP rates in coniferous forests were significantly lower (2.56 ton C ha^{-1} y^{-1}), especially in the spring and summer months.

Agricultural areas showed strong differences in NPP rates between Crops and Grasslands (Figure 10). Overall, the variation in NPP rates across the year followed the same trend as in forest classes: highest variability between March and April, stable NPP rates until July, and continuous decrease until December; but in this case never reaching the absolute zero productivity on average. Crop types had higher biomass production regularly than grasslands or buffer strips, especially between

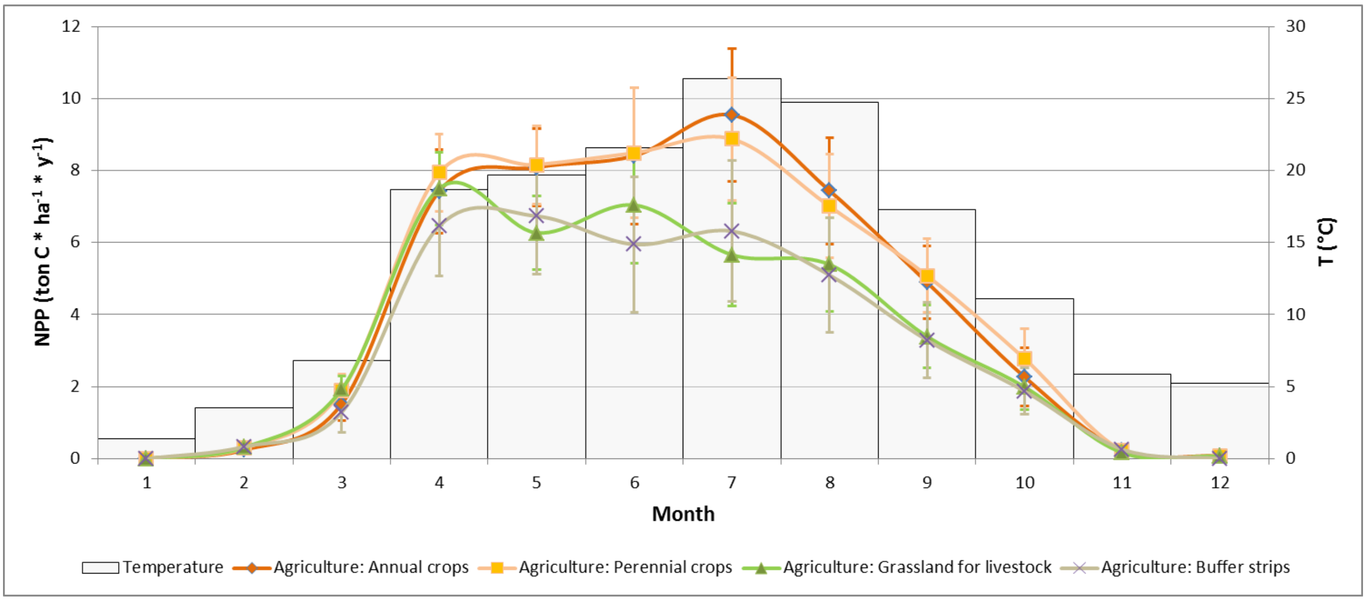

Figure 10: Monthly Net Primary Productivity rates and Temperatures for agricultural land cover types in the Netherlands during the year 2013.

May and September reaching differences of 3.92 ton C ha^{-1} y^{-1}. Crop areas obtained the highest standard deviations during the summer months (1.84 ton C ha^{-1} y^{-1}) due to the differences between crop types across the entire country. Other land cover classes included in the analysis comprised Wetlands, Moors and unpaved surfaces (Figure 11). Their net primary production rates were under the average values, thus meaning lower than agricultural and forested areas. They obtained their highest NPP rates in May being 6.77 ± 1.57, 5.78 ± 1.33, and 5.01 ± 0.98 ton C ha^{-1} y^{-1} respectively. The inter-annual variability was similar to the land cover classes above mentioned, except a decrease in NPP rates on wetlands on June. Wetlands obtained the highest standard deviations considering all land cover classes, showing big spatial differences in their productivity across the Netherlands.

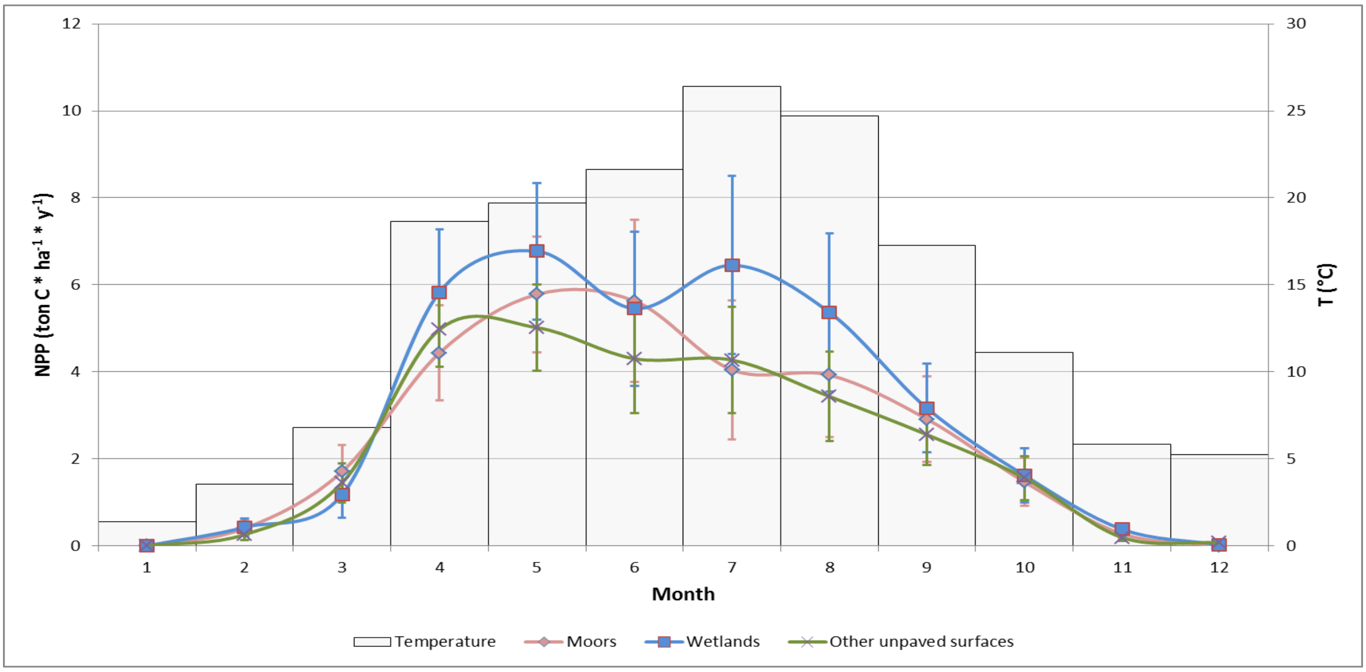

Figure 11: Monthly Net Primary Productivity rates and Temperatures for other land cover types in the Netherlands during the year 2013.

3.2 – Regions

To address the spatial variability in NPP rates across the Netherlands, descriptive statistics were also calculated per province and per municipality (Figure 12).

First, NPP rates variability in provinces showed an increasing trend of vegetation productivity from South to North where the provinces of Groningen (4.50 ton C ha^{-1} y^{-1}), Flevoland (4.34 ton C ha^{-1} y^{-1}) and Noord-Holland (4.31 ton C ha^{-1} y^{-1}) obtained the

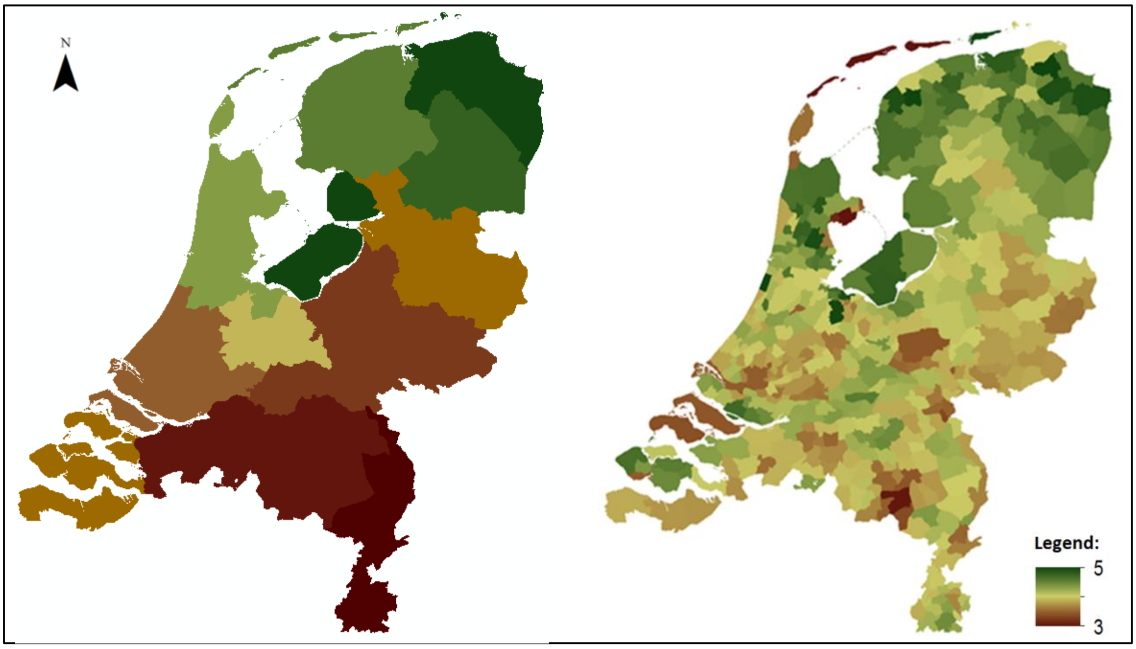

Figure 12: Annual Net Primary Productivity rates per province during the year 2013 on the left; and Annual Net Primary Productivity rates per municipality (ton C ha^{-1} y^{-1}) during the year 2013. On the right

highest rates, while Zeeland (3.87 ton C ha^{-1} y^{-1}), Limburg (3.59 ton C ha^{-1} y^{-1}) and Noord-Brabant (3.55 ton C ha^{-1} y^{-1}) obtained the lowest (Appendix 5). As the NPP rates between provinces varied only 21% of their value, the total carbon uptake by vegetation per province is strongly size-dependent (R^2= 0.891; $p < 0.001$). Then the provinces with larger surfaces such as Gelderland (142.22 Mton C) and Noord-Brabant (127.77 Mton C), produced more biomass than the smaller ones, like Flevoland (51.88 Mton C) or Utrecht (35.12 Mton C).

Larger variations were observed in the analysis per municipality. Despite the trend South to North is still strong, municipalities with higher impact on the provinces were identified with NPP rates ranging from 5.86 ton C ha^{-1} y^{-1} in municipalities from Groningen in areas dedicated to agriculture, to 1.13 ton C ha^{-1} y^{-1} in the southern part of Noord-Brabant with high coverage of coniferous forest.

In this way, we analyzed each land cover class per province to further identify spatial variations in NPP rates from similar land cover classes (Figure 13). First, results showed that deciduous forests had the highest annual rates in northern provinces such as Groningen (6.75 ton C ha^{-1} y^{-1}), Friesland (6.63 ton C ha^{-1} y^{-1}) and Flevoland (6.61 ton C ha^{-1} y^{-1}), while coniferous forest produced more biomass in Groningen (3.15 ton C ha^{-1} y^{-1}), but also in southern provinces like Zuid-Holland (2.54 ton C ha^{-1} y^{-1}) or Zeeland (2.47 ton C ha^{-1} y^{-1}). Deciduous forest accumulated 9.14 Mtons C and coniferous forest 6.41 Mtons C in Gelderland, which was the province with the most forest surface. Crops were also more productive in the north part of the country (Friesland: 5.42 ton C ha^{-1} y^{-1}) and less productive in the south-west (Zeeland: 4.46 ton C ha^{-1} y^{-1}). Other land cover classes presented small differences in their spatial distribution excluding the wetlands in Flevoland, which obtained NPP rates (4.99 ton C ha^{-1} y^{-1}) in an area mainly dominated by agricultural lands.

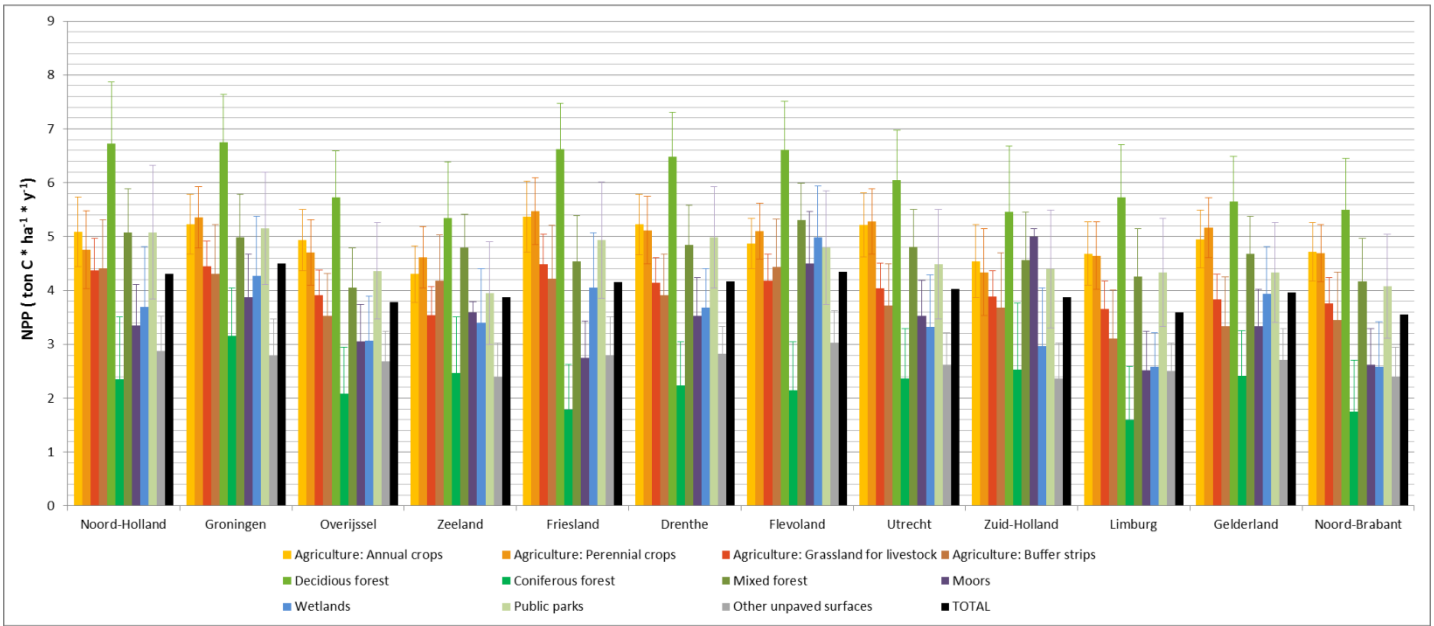

Figure 13: Annual Net Primary Productivity rates per land cover type per province in the Netherlands during the year 2013.

4 – Discussion

4.1 – Model

The results and validity of this approach was achieved based on the EU_NL map, which has incorporated high resolution and it is the most reliable input of the model. Other inputs such as f_{APAR} and LAI products from MOD15A3H were selected due to their 500m spatial resolution, higher than similar products from other satellites, which normally provide this data at 1km resolution. In the case of temperature datasets, we assumed low spatial variation between temperatures. This assumption allowed us to use the daily temperature datasets from MODIS at 1km resolution and rescale them to our goals. The DSSF data from LAF-SAT was also obtained with a resolution of 1km. Despite irradiation on the surface is also continuous and variations under this 1km grid are unremarkable, it has been the main source of underestimation of NPP in the northern islands of Friesland province due to their small scale and distance from the mainland.

Other important factor driving productivity and respiration processes is the temperature variability. The temperature data from MODIS is highly validated globally with resolution of 1km (Wan, 2008). But national and local daily climatic datasets would further improve the accuracy of the predictions and decrease the periodicity of the products (Neumann et al., 2015). Obtaining local climate data may not only include daily temperatures to account precisely for the temperature stress in carbon uptake and respiration processes, but also other variables such as vapour pressure deficit and rainfall rates to point at evapotranspiration and water stresses that affect vegetation (Gilabert et al., 2015).

However, we found large scale spatial variation in NPP rates due to temperature variability and surface radiation (Chu et al., 2016) and also local variations regarding land cover types. This scale is crucial to consider possible sources of uncertainty and, in this way, produce sound information for further development of the model.

4.2 – Uncertainty

The sources of uncertainty from this remote sensing approach have been identified and can be divided between spatial and temporal uncertainties.

Spatial uncertainty is commonly found in remote sensing approaches due to the inevitable generalization to a certain degree. In our case study, the main source of spatial uncertainty emerged from the land cover classification from the EU_NL map. Even though the EU_NL map has a high resolution of 10m, some categories such as dunes or sand areas might have been underestimated. The classification does not make distinctions between dunes with permanent grass and sandy dunes, and does not recognize sparse vegetation in sandy areas. This substantially affects the NPP rates of these areas, which obtain values of 0 in the products, thus not offering a realistic representation of carbon uptake in these land cover types. This also becomes visible in urban landscapes where the current LAI and f_{APAR} inputs offer no data values leading to lack of information from the productivity in urban vegetation. Correcting data gaps in urban areas and improving urban vegetation maps with ground-based inventories can improve the performance of the modelled estimations for urban areas (Stronbach et al., 2012). This improvement should be feasible in the short term using the new vegetation map from RIVM, which includes urban sub-pixel information.

The other representative source of spatial uncertainty is given in the equivalence table of land cover categories (Appendix 4). In order to assign static parameters to EU_NL land cover classes they were coupled to the 8 land cover types of the land cover classification system from the University of Maryland (UMD_VEG_LC), which included parametrizations of ε, SLA, or tissue ratios. UMD_VEG_LC is the land cover classification driving the BPLUT and conceptually driving algorithm of MOD17 for NPP estimations. Including more specific land cover classes in the BPLUT (Appendix 1), or refining those parameters for particular species would allow better estimations from the algorithm. For instance, croplands are assumed to be only one category with the same parameters disregarding distinctions between annual and perennial, or fruit trees and corn fields. Even though this statement may lead to under/overestimation of NPP rates, differences in between crop types can be appreciated from their reflectance wavelengths included in the algorithm and should be analyzed in further studies.

Sources of temporal uncertainty have to be taken into consideration. From this perspective, monthly measurements provide useful information about effects of seasonality on vegetation productivity and a useful general view of C uptake variability across the year. But it is possible that stochastic climatic events such as floods, exceptional heat, or droughts affect NPP at smaller temporal scales (Ciais et al., 2005). Management techniques such as mowing or harvesting also occur at smaller temporal scales as can be seen in Figure 10, where observable fluctuations in grasslands occur during the spring and summer months. Composites of 8-days periods of f_{APAR} and LAI can be obtained from MOD15A3H, also DSSF and Temperatures can be obtained hourly. Therefore, considering a possible reduction to daily or weekly products can be helpful to assess the effects of individual events.

Nevertheless, NPP variations should be considered in the long term to address climate change effects on biomass production and carbon sequestration. The products of this model can be obtained with the same spatial and temporal resolution for the period 2000-2016, which can already offer a good overview of the carbon flows across the first decades of this century. Reporting changes at this scale can also offer relevant information in vegetation growth, turnover rates, and the comparison of different management strategies.

Although there are multiple uncertainty sources, these have a low impact in the final product due to the high quality of the input data and the strong reliability on the land cover map (Kicklighter et al., 1999). Our results show a strong agreement with other remote sensing approaches, in-situ measurements, and process-based models estimating NPP in local or broader scales.

Forests have the most reported NPP rates modelled in Europe. Our annual average NPP results for forest in the Netherlands accounted rates of 5.32 ± 2.57 ton C ha^{-1} yr^{-1}. Neumann et al. (2016) reported biomass NPP values for European forest of 6.66 ± 2.52 ton C ha^{-1} yr^{-1} based on MODIS EURO. That study also pointed out overestimations of up to 16% compared with the results of national forest inventory data, which leave our products closer to forest ground level NPP measurements of 5.61 ± 4.12 ton C ha^{-1} yr^{-1}. Luyssaert et al. (2009) also reported NPP comparisons of European forests between different models ranging from 4.38 ± 1.12 to 6.17 ± 2.55 ton C ha^{-1} yr^{-1}. Concerning the products of these different carbon models our approach has more similarities with national forest inventories and BIOME-BGC model.

Croplands in Europe have also reported NPP rates in different models according to our results. MODIS estimated biomass NPP in European croplands on 5.10 ton C ha^{-1} yr^{-1}, while other models such as CASA or LPJml calculated an average value of 4.81 ton C ha^{-1} yr^{-1}, which is more in agreement with our results for 2013 (4.21 ± 2.11 ton C ha^{-1} yr^{-1}), and also in accordance with the findings of Ciais et al. (2010). Nevertheless broader scale studies such as Monfreda et al. 2000 have reported values of 3.41 ton C ha^{-1} yr^{-1} for European croplands, meaning the crop productivity in the Netherlands surpasses the European average.

Our model also produced annual NPP rates of 3.31 ± 1.61 ton C ha^{-1} yr^{-1} for grasslands in the Netherlands. These values also highly agree with observed NPP measurements and differ from other process-based models that have estimated NPP in European grasslands, which commonly err on the side of overestimation. Hussain et al. (2011) found NPP rates of 4.01 ton C ha^{-1} yr^{-1} in German temperate grasslands, while other models include overestimations from in-situ measurements from 30 to 50% due to parametrization uncertainty (Chang et al. 2015).

Despite there are lack of references from in-situ NPP measurements or small scale measurements for the Netherlands to compare current results, there is a strong agreement with literature for the European NPP rates of the different land cover classes analyzed. This allows further intercomparison between classes and reliable estimates of biomass productivity.

4.3 – Applications

This satellite-based model is also meant to be a support tool for spatial planning because it offers a wide range of applications in the policy and management perspectives. Accordingly, several models from the Atlas of Natural Capital can benefit from this algorithm to support the current transition into a circular economy in the Netherlands, which demands specific and broad scale accounting of current ecosystem services. Among these services, this algorithm improve the biomass production service modelling biomass stocks and growth, which embraces multiple applications such as estimates of the amount of fodder produced in grasslands or the amount of wood provided by forests. This model is also beneficial for the accounts of biomass for energy purposes, allowing to estimate, for instance, the amount of biomass being produced at road sides, or the biomass considered as crop residues for the bio-based economy. Statistics Netherlands is currently including several products from this model to improve the Dutch ecosystem accounts.

Additionally, this model provides estimations on CO_2 sequestration quantifying carbon uptake of biomass that can be used in national or regional management plans to reduce atmospheric CO_2 concentrations and meet climate change goals.

Monthly products offer a sound insight to quantify the last fluctuations and current state of vegetation through time series of NPP. These time series can be also analyzed to estimate future trends in carbon capture and biomass supply, allowing to design scenarios under different pressures (Reyer et al., 2013), and strategies to comply with environmental requirements and developments. As an example, this becomes applicable in the recent goal that the Netherlands has stated of expanding the forested areas (Actieplan Bos en Hout, 2016). Then, the application of forest products resulting from this model can ensure successful locations in this context.
Valuating vegetation flows also give the possibility to point at disturbances and quantify their correlated damages or benefits for the different vegetation types. In this way land cover changes, decreasing crop production, or forest depletion can be easily identified and amended.

5 – Conclusions

This study introduces a satellite-based model that offers novel insights for vegetation productivity in the Netherlands at 10m resolution for the year 2013. The model optimizes previous approaches downscaling NPP for all the vegetation types in the Netherlands. Satellite-based estimations were lacking enough spatial and temporal resolution in this country, and current satellite products allow to produce continuous spatial and temporal data with high performance results.

The model is conceptually based on MOD17 algorithm, exchanging model inputs into higher resolution data, and as result we have decrease uncertainty in all land cover classes and found strong agreement with empirical measurements and specialized literature. Large variability in NPP rates was found in the results, explained by the different monthly climatic conditions across the year 2013 and the biophysical differences between vegetation types.

Validation data for satellite modelling approaches is limited to data availability and comparison with other measurements. Thus, further studies should focus on decreasing spatial uncertainty produced from the input parameters and temporal uncertainty reducing the temporal scale of the products.

This model is oriented to contribute to the carbon accounts of the Netherlands providing quantitative information of vegetation productivity for further modelling ecosystem services in the Atlas Natural Capital (ANK) project. NPP products can be applied to estimate biomass production, human appropriation of net primary production and carbon sequestration identifying inter-annual variability and spatial distribution. Therefore, this approach can be used as a support tool to provide sound advice to policy makers, companies and particulars to ensure efficient and sustainable ecosystem management practices in the transition to circular economy.

6 – References

1. AHLSTROM, A., SCHURGERS, G., ARNETH, A. & SMITH, B. 2012. Robustness and uncertainty in terrestrial ecosystem carbon response to CMIP5 climate change projections. Environmental Research Letters, 7.
2. BEER, C., REICHSTEIN, M., TOMELLERI, E., CIAIS, P., JUNG, M., CARVALHAIS, N., RODENBECK, C., ARAIN, M. A., BALDOCCHI, D., BONAN, G. B., BONDEAU, A., CESCATTI, A., LASSLOP, G., LINDROTH, A., LOMAS, M., LUYSSAERT, S., MARGOLIS, H., OLESON, K. W., ROUPSARD, O., VEENENDAAL, E., VIOVY, N., WILLIAMS, C., WOODWARD, F. I. & PAPALE, D. 2010. Terrestrial Gross Carbon Dioxide Uptake: Global Distribution and Covariation with Climate. Science, 329, 834-838.
3. BERNSTEIN, L., BOSCH, P., CANZIANI, O., CHEN, Z., CHRIST, R., & RIAHI, K. 2008. IPCC, 2007: Climate change 2007: Synthesis report. IPCC.
4. BRAAT, L. C. & DE GROOT, R. 2012. The ecosystem services agenda: bridging the worlds of natural science and economics, conservation and development, and public and private policy. Ecosystem Services, 1, 4-15.
5. CANNELL, M. G. R. & THORNLEY, J. H. M. 2000. Modelling the components of plant respiration: Some guiding principles. Annals of Botany, 85, 45-54.
6. CHANG, J. F., VIOVY, N., VUICHARD, N., CIAIS, P., CAMPIOLI, M., KLUMPP, K., MARTIN, R., LEIP, A. & SOUSSANA, J. F. 2015. Modeled Changes in Potential Grassland Productivity and in Grass-Fed Ruminant Livestock Density in Europe over 1961-2010. Plos One, 10.
7. CHAPIN, F. S., WOODWELL, G. M., RANDERSON, J. T., RASTETTER, E. B., LOVETT, G. M., BALDOCCHI, D. D., CLARK, D. A., HARMON, M. E., SCHIMEL, D. S., VALENTINI, R., WIRTH, C., ABER, J. D., COLE, J. J., GOULDEN, M. L., HARDEN, J. W., HEIMANN, M.,

HOWARTH, R. W., MATSON, P. A., MCGUIRE, A. D., MELILLO, J. M., MOONEY, H. A., NEFF, J. C., HOUGHTON, R. A., PACE, M. L., RYAN, M. G., RUNNING, S. W., SALA, O. E., SCHLESINGER, W. H. & SCHULZE, E. D. 2006. Reconciling carbon-cycle concepts, terminology, and methods. Ecosystems, 9, 1041-1050.

8. CIAIS, P., REICHSTEIN, M., VIOVY, N., GRANIER, A., OGEE, J., ALLARD, V., AUBINET, M., BUCHMANN, N., BERNHOFER, C., CARRARA, A., CHEVALLIER, F., DE NOBLET, N., FRIEND, A. D., FRIEDLINGSTEIN, P., GRUNWALD, T., HEINESCH, B., KERONEN, P., KNOHL, A., KRINNER, G., LOUSTAU, D., MANCA, G., MATTEUCCI, G., MIGLIETTA, F., OURCIVAL, J. M., PAPALE, D., PILEGAARD, K., RAMBAL, S., SEUFERT, G., SOUSSANA, J. F., SANZ, M. J., SCHULZE, E. D., VESALA, T. & VALENTINI, R. 2005. Europe-wide reduction in primary productivity caused by the heat and drought in 2003. Nature, 437, 529-533.
9. CIAIS, P., WATTENBACH, M., VUICHARD, N., SMITH, P., PIAO, S. L., DON, A., LUYSSAERT, S., JANSSENS, I. A., BONDEAU, A., DECHOW, R., LEIP, A., SMITH, P. C., BEER, C., VAN DER WERF, G. R., GERVOIS, S., VAN OOST, K., TOMELLERI, E., FREIBAUER, A., SCHULZE, E. D. & TEAM, C. S. 2010. The European carbon balance. Part 2: croplands. Global Change Biology, 16, 1409-1428.
10. COSTANZA, R., D'ARGE, R., DE GROOT, R., FARBER, S., GRASSO, M., HANNON, B., LIMBURG, K., NAEEM, S., O'NEILL, R. V., PARUELO, J., RASKIN, R. G., SUTTON, P. & VAN DEN BELT, M. 1998. The value of the world's ecosystem services and natural capital (Reprinted from Nature, vol 387, pg 253, 1997). Ecological Economics, 25, 3-15.
11. COSTANZA, R., DE GROOT, R., SUTTON, P., VAN DER PLOEG, S., ANDERSON, S. J., KUBISZEWSKI, I., FARBER, S. & TURNER, R. K. 2014. Changes in the global value of ecosystem services. Global Environmental Change-Human and Policy Dimensions, 26, 152-158.
12. CROSSMAN, N. D., BURKHARD, B., NEDKOV, S., WILLEMEN, L., PETZ, K., PALOMO, I., DRAKOU, E. G., MARTIN-LOPEZ, B., MCPHEARSON, T., BOYANOVA, K., ALKEMADE, R., EGOH, B., DUNBAR, M. B. & MAES, J. 2013. A blueprint for mapping and modelling ecosystem services. Ecosystem Services, 4, 4-14.
13. DE GROOT, R. S., WILSON, M. A. & BOUMANS, R. M. J. 2002. A typology for the classification, description and valuation of ecosystem functions, goods and services. Ecological Economics, 41, 393-408.
14. DEFRIES, R. S., FIELD, C. B., FUNG, I., COLLATZ, G. J. & BOUNOUA, L. 1999. Combining satellite data and biogeochemical models to estimate global effects of human-induced land cover change on carbon emissions and primary productivity. Global Biogeochemical Cycles, 13, 803-815.
15. GARBULSKY, M. F., PENUELAS, J., PAPALE, D., ARDO, J., GOULDEN, M. L., KIELY, G., RICHARDSON, A. D., ROTENBERG, E., VEENENDAAL, E. M. & FILELLA, I. 2010. Patterns and controls of the variability of radiation use efficiency and primary productivity across terrestrial ecosystems. Global Ecology and Biogeography, 19, 253-267.
16. GOWER, S. T., KUCHARIK, C. J. & NORMAN, J. M. 1999. Direct and indirect estimation of leaf area index, f(APAR), and net primary production of terrestrial ecosystems. Remote Sensing of Environment, 70, 29-51.

17. HUSSAIN, M. Z., GRUNWALD, T., TENHUNEN, J. D., LI, Y. L., MIRZAE, H., BERNHOFER, C., OTIENO, D., DINH, N. Q., SCHMIDT, M., WARTINGER, M. & OWEN, K. 2011. Summer drought influence on CO2 and water fluxes of extensively managed grassland in Germany. Agriculture Ecosystems & Environment, 141, 67-76.
18. IMHOFF, M. L., BOUNOUA, L., RICKETTS, T., LOUCKS, C., HARRISS, R. & LAWRENCE, W. T. 2004. Global patterns in human consumption of net primary production. Nature, 429, 870-873.
19. ITO, A. 2011. A historical meta-analysis of global terrestrial net primary productivity: are estimates converging? Global Change Biology, 17, 3161-3175.
20. KICKLIGHTER, D. W., BONDEAU, A., SCHLOSS, A. L., KADUK, J., MCGUIRE, A. D. & PARTICIPANTS POTSDAM, N. P. P. M. I. 1999. Comparing global models of terrestrial net primary productivity (NPP): global pattern and differentiation by major biomes. Global Change Biology, 5, 16-24.
21. LAL, R. 2008. Sequestration of atmospheric CO2 in global carbon pools. Energy & Environmental Science, 1, 86-100.
22. LSA-SAF 2011a. Product user manual Down-welling Surface Shortwave Flux (DSSF). Ref: SAF/LAND/MF/PUM_DSSF/2.6v2. Available online at: http://landsaf.meteo.pt.
23. LSA-SAF 2011b. Validation report Down-welling Surface Shortwave Flux (DSSF). Ref: *SAF/LAND/MF/VR_DSSF/I_11v4*. Available online at: http://landsaf.meteo.pt.
24. LUYSSAERT, S., CIAIS, P., PIAO, S. L., SCHULZE, E. D., JUNG, M., ZAEHLE, S., SCHELHAAS, M. J., REICHSTEIN, M., CHURKINA, G., PAPALE, D., ABRIL, G., BEER, C., GRACE, J., LOUSTAU, D., MATTEUCCI, G., MAGNANI, F., NABUURS, G. J., VERBEECK, H., SULKAVA, M., VAN DER WERF, G. R., JANSSENS, I. A. & TEAM, C.-I. S. 2010. The European carbon balance. Part 3: forests. Global Change Biology, 16, 1429-1450.
25. MATSUSHITA, B. & TAMURA, M. 2002. Integrating remotely sensed data with an ecosystem model to estimate net primary productivity in East Asia. Remote Sensing of Environment, 81, 58-66.
26. MELILLO, J. M., MCGUIRE, A. D., KICKLIGHTER, D. W., MOORE, B., VOROSMARTY, C. J. & SCHLOSS, A. L. 1993. GLOBAL CLIMATE-CHANGE AND TERRESTRIAL NET PRIMARY PRODUCTION. Nature, 363, 234-240.
27. Millennium Ecosystem Assessment, Ecosystems and Human Wellbeing: A Framework for Assessment 2003. Island Press.
28. MONFREDA, C., RAMANKUTTY, N. & FOLEY, J. A. 2008. Farming the planet: 2. Geographic distribution of crop areas, yields, physiological types, and net primary production in the year 2000. Global Biogeochemical Cycles, 22.
29. MONTEITH, J. L. 1972. SOLAR-RADIATION AND PRODUCTIVITY IN TROPICAL ECOSYSTEMS. Journal of Applied Ecology, 9, 747-766.
30. MORENO, A., NEUMANN, M., ZHAO, M., & HASENAUER, H. 2015. Calculating Regional MODIS NPP for Europe. EGU General Assembly Conference Abstracts , 17, 74.
31. NEMANI, R. R., KEELING, C. D., HASHIMOTO, H., JOLLY, W. M., PIPER, S. C., TUCKER, C. J., MYNENI, R. B. & RUNNING, S. W. 2003. Climate-driven increases in global terrestrial net primary production from 1982 to 1999. Science, 300, 1560-1563.
32. Netherlands, CBS Statistics. Ministry of Health, Welfare and Sports.

33. NEUMANN, M., MORENO, A., THURNHER, C., MUES, V., HARKONEN, S., MURA, M., BOURIAUD, O., LANG, M., CARDELLINI, G., THIVOLLE-CAZAT, A., BRONISZ, K., MERGANIC, J., ALBERDI, I., ASTRUP, R., MOHREN, F., ZHAO, M. & HASENAUER, H. 2016. Creating a Regional MODIS Satellite-Driven Net Primary Production Dataset for European Forests. Remote Sensing, 8.
34. NEUMANN, M., ZHAO, M. S., KINDERMANN, G. & HASENAUER, H. 2015. Comparing MODIS Net Primary Production Estimates with Terrestrial National Forest Inventory Data in Austria. Remote Sensing, 7, 3878-3906.
35. PACHAURI, R. K., MEYER, L., PLATTNER, G. K., & STOCKER, T. 2015. IPCC, 2014: Climate Change 2014: Synthesis Report. IPCC.
36. REYER, C. P., LEUZINGER, S., RAMMIG, A., WOLF, A., BARTHOLOMEUS, R. P., BONFANTE, A., DE LORENZI, F., DURY, M., GLINING, P., JAOUDE, R. A. & KLEIN T. 2013. A plant's perspective of extremes: terrestrial plant responses to changing climatic variability. Global change biology, 19(1), 75-89.
37. RUNNING, S. W., & ZHAO, M. 2015. User’s guide daily GPP and annual NPP (MOD17A2/A3) products NASA earth observing system MODIS land algorithm. Available online at: http://ntsg.umt.edu/sites/ntsg.umt.edu/files/modis/MOD17UsersGuide2015_v3.pdf .
38. RUNNING, S. W., NEMANI, R. R., HEINSCH, F. A., ZHAO, M. S., REEVES, M. & HASHIMOTO, H. 2004. A continuous satellite-derived measure of global terrestrial primary production. Bioscience, 54, 547-560.
39. RYAN, M. G. 1991. A SIMPLE METHOD FOR ESTIMATING GROSS CARBON BUDGETS FOR VEGETATION IN FOREST ECOSYSTEMS. Tree Physiology, 9, 255-266.
40. SALA, O. E. , JACKSON, R. B., MOONEY, H. A. & HOWARTH, R. W. 2000. Methods in ecosystem science. Springer-Verlag.
41. SAMANTA, A., GANGULY, S., & MYNENI, R. B. 2011. MODIS Enhanced Vegetation Index data do not show greening of Amazon forests during the 2005 drought. New Phytologist, 189(1), 11-15.
42. SCHMETZ, J., PILI, P., TJEMKES, S., JUST, D., KERKMANN, J., ROTA, S. & RATIER, A. 2002. An introduction to Meteosat Second Generation (MSG). Bulletin of the American Meteorological Society, 83, 977-+.
43. STROHBACH, M. W. & HAASE, D. 2012. Above-ground carbon storage by urban trees in Leipzig, Germany: Analysis of patterns in a European city. Landscape and Urban Planning, 104, 95-104.
44. THORNTON, P. E. 2000. User’s Guide for BIOME-BGC, version 4.1. 1. Available online at: ftp://daac.ornl.gov/data/model_archive/BIOME_BGC/biome_bgc_4.1.1/comp/bgc_users_guide_411.pdf.
45. TJOELKER, M. G., OLEKSYN, J. & REICH, P. B. 2001. Modelling respiration of vegetation: evidence for a general temperature-dependent Q(10). Global Change Biology, 7, 223-230.
46. UNITED NATIONS ENVIRONMENT PROGRAMME (UNEP) 2013. Global Environment Outlook 2000. Routledge.

47. VILE, D., GARNIER, E., SHIPLEY, B., LAURENT, G., NAVAS, M. L., ROUMET, C., LAVOREL, S., DIAZ, S., HODGSON, J. G., LLORET, F., MIDGLEY, G. F., POORTER, H., RUTHERFORD, M. C., WILSON, P. J. & WRIGHT, I. J. 2005. Specific leaf area and dry matter content estimate thickness in laminar leaves. Annals of Botany, 96, 1129-1136.
48. WAN, Z. M. 2008. New refinements and validation of the MODIS Land-Surface Temperature/Emissivity products. Remote Sensing of Environment, 112, 59-74.
49. WAN, Z., ZHANG, Y., ZHANG, Q. & LI, Z. L. 2004. Quality assessment and validation of the MODIS global land surface temperature. International Journal of Remote Sensing, 25, 261-274.
50. XIAO, X. M., HOLLINGER, D., ABER, J., GOLTZ, M., DAVIDSON, E. A., ZHANG, Q. Y. & MOORE, B. 2004. Satellite-based modeling of gross primary production in an evergreen needleleaf forest. Remote Sensing of Environment, 89, 519-534.
51. YAN, K., PARK, T., YAN, G. J., LIU, Z., YANG, B., CHEN, C., NEMANI, R. R., KNYAZIKHIN, Y. & MYNENI, R. B. 2016. Evaluation of MODIS LAI/FPAR Product Collection 6. Part 2: Validation and Intercomparison. Remote Sensing, 8.
52. YANG, W. Z., TAN, B., HUANG, D., RAUTIAINEN, M., SHABANOV, N. V., WANG, Y., PRIVETTE, J. L., HUEMMRICH, K. F., FENSHOLT, R., SANDHOLT, I., WEISS, M., AHL, D. E., GOWER, S. T., NEMANI, R. R., KNYAZIKHIN, Y. & MYNENI, R. B. 2006. MODIS leaf area index products: From validation to algorithm improvement. Ieee Transactions on Geoscience and Remote Sensing, 44, 1885-1898.
53. ZHAO, M. S. & RUNNING, S. W. 2010. Drought-Induced Reduction in Global Terrestrial Net Primary Production from 2000 Through 2009. Science, 329, 940-943.
54. ZHAO, M. S., HEINSCH, F. A., NEMANI, R. R. & RUNNING, S. W. 2005. Improvements of the MODIS terrestrial gross and net primary production global data set. Remote Sensing of Environment, 95, 164-176.
55. ZHAO, M. S., RUNNING, S., HEINSCH, F. A., & NEMANI, R. 2010. MODIS-derived terrestrial primary production. Land Remote Sensing and Global Environmental Change: NASA's earth observing system and the science of ASTER and MODIS, 635-660.

Appendix 1 – Biome-Property-Look-Up-Table (BPLUT)

Biome-Property-Look-Up-Table (BPLUT) including model static set-up parameters from MOD17 algorithm applied to CBS Land cover classes (EU_NL). The classification system corresponds with the CBS land cover classes summarized In Appendix 4.

	ε	SLA	$Leaf_{RESP-BASE}$	$Root_{RESP-BASE}$	Root-$Leaf_{RATIO}$	$Wood_{RESP-BASE}$	Wood-$Leaf_{RATIO}$	T_{MAX}	T_{MIN}
Units	kg C MJ^{-1}	m^2 kg C^{-1}	kg C kg C^{-1} day^{-1}	kg C kg C^{-1} day^{-1}	-	kg C kg C^{-1} day^{-1}	-	°C	°C
1	0.001044	30.4	0.0098	0.00819	2	0	-	12.02	-8
2	0.001044	30.4	0.0098	0.00819	2	0	-	12.02	-8
3	0	0	0	0	0	0	-	-	-
4	0.00086	37.5	0.0098	0.00819	2.6	0	-	12.02	-8
5	0.001281	9	0.00869	0.00519	1	0.00436	0.079	8.61	-8
6	0	0	0	0	-	0	-	-	-
11	0.00086	37.5	0.0098	0.00819	2.6	0	-	12.02	-8
12	0.000841	11.5	0.00519	0.00519	1.3	0.00218	0.04	8.8	-8
21	0.001165	21.8	0.00778	0.00519	1.1	0.00371	0.203	9.94	-6
22	0.000962	14.1	0.00604	0.00519	1.2	0.00397	0.182	8.31	-8
23	0.001051	21.5	0.00778	0.00519	1.1	0.00371	0.203	9.5	-7
24	0.001281	9	0.00869	0.00519	1	0.00436	0.079	8.61	-8
25	0	0	0	0	-	0	-	-	-
26	0.001281	9	0.00869	0.00519	1	0.00436	0.079	8.61	-8
27	0.00086	37.5	0.0098	0.00819	2.6	0	-	12.02	-8
28	0.001051	21.5	0.00778	0.00519	1.1	0.00371	0.203	9.5	-7
29	0.000841	11.5	0.00519	0.00519	1.3	0.00218	0.04	8.8	-8
31	0.000841	11.5	0.00519	0.00519	1.3	0.00218	0.04	8.8	-8
32	0.000841	11.5	0.00519	0.00519	1.3	0.00218	0.04	8.8	-8
41	0	0	0	0	-	0	-	-	-
42	0	0	0	0	-	0	-	-	-
51	0	0	0	0	-	0	-	-	-
52	0	0	0	0	-	0	-	-	-
53	0	0	0	0	-	0	-	-	-
999	0	0	0	0	-	0	-	-	-

Appendix 2 – Model Scheme

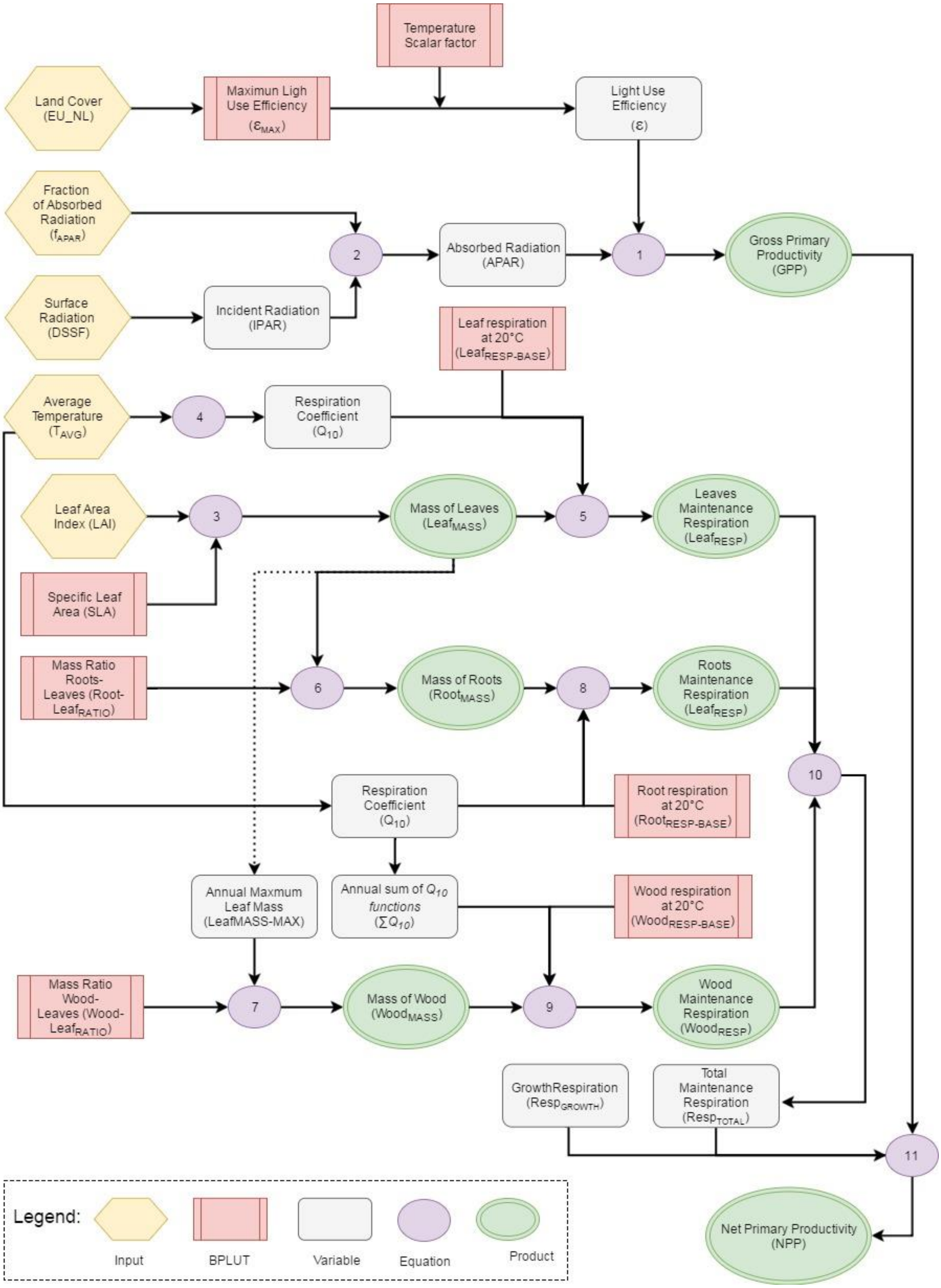

Appendix 3 – Parameters and equations

Parameter	Units	Description	Source	Scale factor
$Leaf_{MASS-MAX}$	kg C * m^{-2}	Maximum leaf mass during the year	$Leaf_{MASS}$	-
APAR	MJ * m^{-2} * day^{-1}	Absorbed PAR on vegetation	Equation 2	-
DSSF	J * m^{-2} * day^{-1}	Downward Surface Shortwave Flux (daily/ 1Km2)	EUMETSAT	10
EU_NL	m^2	Land cover map of the Netherlands ($10m^2$)	CBS	-
f_{APAR}	Percent	Fraction of Photosynthetically Active Radiation (500 m^2)	MODIS Terra	0.01
$Root\text{-}Leaf_{RATIO}$	None	Ratio of fine root carbon to leaf carbon	BPLUT	-
$Root_{MASS}$	kg C * m^{-2}	Fine roots mass	Equation 6	-
$Root_{RESP}$	kg C * day^{-1}	Maintenance respiration of fine roots	Equation 8	-
$Root_{RESP-BASE}$	kg C * kg C^{-1} day^{-1}	Maintenance respiration per unit fine root carbon per day at 20 °C	BPLUT	-
GPP	kg C * m^{-2} * day^{-1}	Gross Primary Productivity	Equation 1	-
IPAR	MJ * m^{-2} * day^{-1}	Incident PAR on vegetation	DSSF * 0.45	-
LAI	m2 * m-2	Leaf Area Index (500m2)	MODIS	0.1
$Leaf_{MASS}$	kg C * m^{-2}	Leaf mass	Equation 3	-
$Leaf_{RESP}$	kg C * day^{-1}	Maintenance respiration of leaves	Equation 5	-
$Leaf_{RESP-BASE}$	kg C * kg C^{-1} * day^{-1}	Maintenance respiration per unit leaf carbon per day at 20 °C	BPLUT	-
$Wood\text{-}Leaf_{RATIO}$	None	Ratio of wood carbon to annual maximum leaf carbon	BPLUT	-
$Wood_{MASS}$	kg C * m^{-2}	Mass of living wood	Equation 7	-
$Wood_{RESP}$	kg C * day^{-1}	Maintenance respiration of wood	Equation 9	-
$Wood_{RESP-BASE}$	kg C * kg C^{-1} * day^{-1}	Maintenance respiration per unit wood carbon per day at 20 °C	BPLUT	-
ε	kg C * MJ^{-1}	The radiation conversion efficiency adapted to climatic conditions	T function	-
ε_{max}	kg C * MJ^{-1}	The maximum radiation conversion efficiency	BPLUT	-
NPP	Tons * ha * year	Net Primary Productivity	Equation 11	-
Q_{10}	None	Exponent shape parameter controlling respiration as a function of temperature	BPLUT	-
SLA	m^2 * kg C^{-1}	Projected leaf area per unit mass of leaf carbon	BPLUT	-
T_{AVG}	°C	Average daily Temperature	MODIS	0.02
T_{MIN}	°C	Temperature at which GPP is 0	BPLUT	-
T_{MAX}	°C	Temperature from which GPP is optimal	BPLUT	-
$Resp_{TOTAL}$	kg C * day^{-1}	Sum of maintenance respirations from leaves, fine roots, and wood.	Equation 10	-

Equation	Formula
1	$GPP = \varepsilon * APAR\ T_{MAX}\ T_{MIN}$
2	$APAR = IPAR * f_{APAR}$
3	$Leaf_{MASS} = LAI / SLA$
4	$Q_{10} = 3.22 – 0.046 * Tavg$
5	$Leaf_{RESP} = Leaf_{MASS} * Leaf_{RESP\text{-}BASE} * Q_{10}\ [(Tavg - 20.0) / 10.0]$
6	$Root_{MASS} = Leaf_{MASS} * Root\text{-}Leaf_{RATIO}$
7	$Wood_{MASS} = Leaf_{MASS\text{-}MAX} * Wood\text{-}Leaf_{RATIO}$
8	$Root_{RESP} = Root_{MASS} * Root_{RESP\text{-}BASE} * Q_{10}\ [(T_{AVG} - 20.0) / 10.0]$
9	$Wood_{RESP} = Wood_{MASS} * Wood_{RESP\text{-}BASE} * \sum Q_{10}\ [(T_{AVG}-20.0)/10.0]$
10	$Resp_{TOTAL} = Leaf_{RESP} + Root_{RESP} + Wood_{RESP}$
11	$NPP = 0.8 * (GPP- Resp_{TOTAL})$

Appendix 4 - Equivalence table of land cover categories

	CBS Land cover classes		MODIS Land cover classes
1	Agriculture: Annual crops	1	Croplands
2	Agriculture: Perennial crops	1	
3	Greenhouses	0	0
4	Agriculture: Grassland for livestock	2	Grassland
5	Agriculture: Buffer strips	4	Closed Shrublands
6	Agriculture: Built	0	0
11	Dunes with permanent grass	2	Grassland
12	Beach. sandbanks and dunes	3	Open Shrublands
21	Decidious forest	5	Deciduous Broadleaf Forest
22	Coniferous forest	6	Evergreen Needleleaf Forest
23	Mixed forest	7	Mixed forests
24	Moors	4	Closed Shrublands
25	Sand	0	0
26	Wetlands	4	Closed Shrublands
27	Grasslands. without pasture	2	Grassland
28	Public parks		Mixed forests
29	Other unpaved surfaces	3	Open Shrublands
31	Floodplains	3	
32	Salt marshes	3	
41	Residential	0	0
42	Built Areas	0	
51	Sea	0	
52	Lakes. ponds and other inland waters	0	
53	Rivers	0	
999	Unknown	0	

Appendix 5 – Monthly NPP in 2013

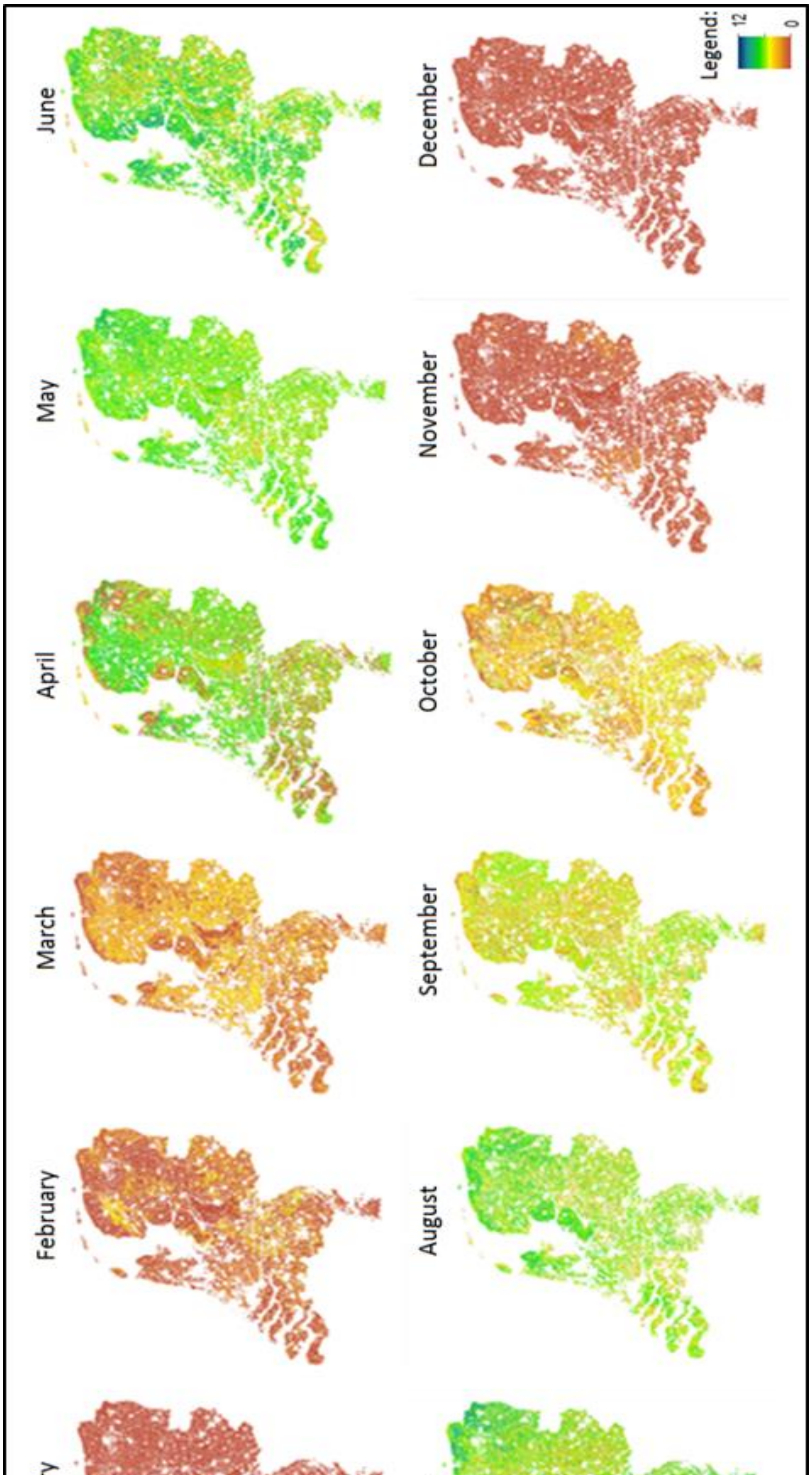

Monthly NPP in 2013 at 10m resolution in ton C ha^{-1} y^{-1}.

Appendix 6 – Mean NPP and Total carbon uptake

		Noord-Holland	Groningen	Overijssel	Zeeland	Friesland	Drenthe
Agriculture: Annual crops	Mean	5.09	5.23	4.93	4.30	5.37	5.22
	STD	1.30	1.12	1.13	1.04	1.31	1.11
	Total	19.55	49.67	25.99	40.38	21.66	41.78
Agriculture: Perennial crops	Mean	4.76	5.36	4.70	4.62	5.47	5.12
	STD	1.46	1.14	1.22	1.13	1.24	1.25
	Total	5.43	0.99	2.07	2.44	0.47	2.37
Agriculture: Grassland for livestock	Mean	4.38	4.45	3.91	3.54	4.49	4.14
	STD	1.19	0.93	0.93	1.08	1.10	0.96
	Total	27.97	27.81	52.81	5.13	78.24	27.22
Agriculture: Buffer strips	Mean	4.41	4.30	3.52	4.18	4.22	3.91
	STD	1.81	1.84	1.58	1.69	1.97	1.53
	Total	1.12	2.07	1.14	1.59	3.44	1.91
Decidious forest	Mean	6.72	6.75	5.73	5.35	6.63	6.48
	STD	2.30	1.79	1.72	2.08	1.68	1.65
	Total	3.86	3.23	7.02	1.73	4.78	6.84
Coniferous forest	Mean	2.36	3.15	2.08	2.47	1.79	2.23
	STD	1.13	1.64	1.25	1.47	1.33	1.11
	Total	0.25	0.04	1.50	0.07	0.30	1.81
Mixed forest	Mean	5.07	4.98	4.06	4.79	4.54	4.84
	STD	1.64	1.61	1.47	1.25	1.70	1.47
	Total	1.44	0.39	5.71	0.11	1.36	5.48
Moors	Mean	3.35	3.87	3.05	3.60	2.75	3.53
	STD	1.51	1.62	1.37	0.38	1.36	1.41
	Total	0.38	0.05	1.30	0.00	0.72	3.13
Wetlands	Mean	3.69	4.27	3.07	3.40	4.05	3.68
	STD	2.25	2.20	1.65	2.01	2.04	1.43
	Total	0.01	0.03	0.02	0.01	0.02	0.01
Public parks	Mean	5.08	5.16	4.37	3.96	4.93	4.99
	STD	2.49	2.08	1.79	1.91	2.16	1.88
	Total	2.50	0.98	1.41	0.88	1.47	1.50
Other unpaved surfaces	Mean	2.88	2.79	2.69	2.39	2.80	2.83
	STD	1.28	1.35	1.11	1.26	1.42	1.02
	Total	2.57	1.06	1.02	0.99	1.31	1.16
Floodplains	Mean	3.94	3.69	3.35	0.00	2.81	2.98
	STD	0.36	0.83	0.68	0.00	0.40	0.35
	Total	0.00	0.00	0.00	0.00	0.00	0.00
TOTAL	Mean	4.31	4.50	3.79	3.87	4.15	4.16
	Total	65.07	86.32	99.99	53.33	113.77	93.21

**Mean and STD in ton C ha^{-1} y^{-1}; Total in Mton C y^{-1}*

		Flevoland	Utrecht	Zuid-Holland	Limburg	Gelderland	Noord-Brabant
Agriculture: Annual crops	Mean	4.87	5.22	4.55	4.69	4.95	4.71
	STD	0.93	1.19	1.35	1.19	1.08	1.09
	Total	33.37	3.51	18.83	24.44	31.66	57.03
Agriculture: Perennial crops	Mean	5.10	5.28	4.34	4.65	5.17	4.69
	STD	1.04	1.23	1.61	1.26	1.11	1.06
	Total	3.18	1.36	1.81	3.62	5.61	6.41
Agriculture: Grassland for livestock	Mean	4.19	4.05	3.88	3.66	3.83	3.76
	STD	0.98	0.91	0.97	1.05	0.95	0.95
	Total	4.55	20.87	25.20	10.15	57.65	33.52
Agriculture: Buffer strips	Mean	4.43	3.71	3.69	3.11	3.34	3.45
	STD	1.80	1.56	2.02	1.80	1.82	1.79
	Total	0.46	0.54	1.47	1.08	1.12	2.83
Decidious forest	Mean	6.61	6.05	5.46	5.73	5.65	5.50
	STD	1.81	1.83	2.45	1.96	1.69	1.91
	Total	7.09	2.65	3.13	5.76	9.14	8.64
Coniferous forest	Mean	2.15	2.37	2.54	1.60	2.41	1.75
	STD	1.42	1.08	1.25	1.32	1.14	1.27
	Total	0.07	1.17	0.04	1.08	6.41	4.26
Mixed forest	Mean	5.30	4.81	4.56	4.26	4.69	4.16
	STD	1.36	1.39	1.78	1.79	1.38	1.60
	Total	1.32	2.97	0.07	4.20	20.39	9.23
Moors	Mean	4.50	3.53	4.99	2.52	3.34	2.62
	STD	1.92	1.32	0.31	1.44	1.36	1.34
	Total	0.01	0.44	0.00	0.66	5.86	2.11
Wetlands	Mean	4.99	3.32	2.96	2.58	3.93	2.58
	STD	1.90	1.92	2.18	1.27	1.77	1.69
	Total	0.01	0.00	0.01	0.00	0.01	0.02
Public parks	Mean	4.79	4.49	4.40	4.33	4.34	4.08
	STD	2.11	2.04	2.18	2.01	1.85	1.93
	Total	0.93	0.83	1.89	1.02	2.75	2.20
Other unpaved surfaces	Mean	3.04	2.62	2.36	2.51	2.71	2.40
	STD	1.17	1.17	1.32	1.04	1.14	1.10
	Total	0.90	0.71	1.21	0.91	1.94	1.49
Floodplains	Mean	2.14	2.92	2.73	3.48	3.23	2.90
	STD	0.65	0.90	1.33	0.62	0.93	1.08
	Total	0.00	0.06	0.09	0.00	0.09	0.04
TOTAL	Mean	4.34	4.03	3.87	3.59	3.97	3.55
	Total	51.88	35.12	53.74	52.91	142.62	127.77

**Mean and STD in ton C ha^{-1} y^{-1}; Total in Mton C y^{-1}*